High- and Low-Potential Flavin Mimics. 2. 3,7,10-Trimethyl-(1*H*,3*H*,5*H*,7*H*,9*H*,10*H*)-pyrimido[5,4-*g*]-pteridine-2,4,6,8-tetrone Dianion Reduction of Carbonyl, Nicotinamides, and Alkyl Disulfide Functional Groups

Edward B. Skibo and Thomas C. Bruice*

Contribution from the Department of Chemistry, University of California at Santa Barbara, Santa Barbara, California 93106. *Received August 31, 1982*

Abstract: 3,7,10-Trimethyl-(3*H*,7*H*,9*H*,10*H*)-pyrimido[5,4-*g*]pteridine-2,4,6,8-tetrone (PPT_{ox}) and its conjugate base (PPT_{ox}^-) undergo two-electron reduction to yield 3,7,10-trimethyl-(1*H*,3*H*,5*H*,7*H*,9*H*,10*H*)-pyrimido[5,4-*g*]pteridine-2,4,6,8-tetrone ($PPTH_2$) and its dianion (PPT^{2-}) (Scheme I). The two-electron redox potential $E^{o\prime}$ is 150 mV more negative than that of the corresponding 3-methyllumiflavin (Fl_{ox})/1,5-dihydro-3-methyllumiflavin (FlH_2 + FlH^-) couple. Reductive alkylation of $PPTH_2$ with acetaldehyde (Scheme II) provides the N^5-ethyl derivative of $PPTH_2$ (N^5-EtPPTH$_2$) which is an analogue of the well studied 1,5-dihydro-N^5-ethyl-3-methyllumiflavin (N^5-EtFlH). As in the instance of N^5-EtFlH, N^5-EtPPTH$_2$ can undergo stepwise oxidation to the thermodynamically stable N^5-EtPPT$^{-\cdot}$ radical (analogue of N^5-EtFl·) and hence to the two-electron oxidized species N^5-EtPPT_{ox} (Scheme II). The pK_a for the pseudobase formation via reaction of N^5-EtPPT_{ox} with H_2O (7.34) is compared to the similar pK_a (4.00) for the reaction of N^5-EtFl_{ox}^+ with H_2O. The species PPT_{ox}^- (like Fl_{ox}) is not reduced (H_2O solvent) with $NaCNBH_3$. However, reduction of a solution of PPT_{ox}^- containing formaldehyde with $NaCNBH_3$ yields N^5-MePPT_{ox} and the radical N^5-MePPT$^{-\cdot}$ on admittance of O_2. The mechanism (Scheme III) involves the initial formation of the N^1-carbinolamine of PPT_{ox}^- which when reduced is subject to reductive alkylation at N^5, as in the case of reductive alkylation of $PPTH_2$. The reaction of $PPTH_2$ with formaldehyde has been studied in detail. The reaction resembles, in important details, that for the reaction of FlH_2 with formaldehyde. An initial first-order burst in the formation of PPT_{ox}^- is associated with the competitive reduction of formaldehyde by PPT^{2-} and the formation of the N^5-imine of PPT^{2-} (eq 5; Scheme IV). The latter does not apparently revert readily to carbinolamine, due to its electronic stabilization (structures A, B, C, and D). The N^5-imine of PPT^{2-} is trapped in further reactions to produce compounds with more positive redox potentials than that for the $PPT_{ox}^-/PPTH_2$ couple (possible structures as E, F, etc.). The increase in the rate constant of specific acid catalyzed reduction of formaldehyde by PPT^{2-} ($k = 3.3 \times 10^6$ M^{-2} s^{-1}) over the like constant with FlH^- ($k = 2.3 \times 10^4$ M^{-2} s^{-1}) is related to the difference in the two-electron reduction potential for the two (148 mV) by the free energy relationship 67 mV/Δ log k. The predicted free energy relationship for a series of 1,5-dihydroflavins of varying potentials carrying out reduction of a substrate by two-electron transfer would be 60 mV/Δ log k. Thus, toward formaldehyde, PPT^{2-} exhibits the reactivity of a low-potential FlH^- molecule. The reaction of $PPTH_{2_T}$ (=$PPTH_2$ + PPT^- + PPT^{2-}) with *m*-hydroxybenzaldehyde was studied at pH 5.00 only. In preparative experiments, it was shown that *m*-hydroxybenzaldehyde was reduced to *m*-cresol and a trace of *m*-hydroxybenzyl alcohol and that *m*-hydroxybenzyl alcohol was not an intermediate in the reduction of *m*-hydroxybenzaldehyde to *m*-cresol. The mechanism of Scheme V, which requires 2 equiv of $PPTH_{2_T}$/*m*-hydroxybenzaldehyde, has been suggested. The time course for the formation of PPT_{ox}^- exhibits an initial burst in PPT_{ox}^- formation (10% yield) followed by a slow and multiphasic formation of PPT_{ox}^- to ~100% yield based upon the [$PPTH_{2_T}$] employed. The initial burst in PPT_{ox}^- formation is attributed (as in the case of the formaldehyde reaction) to a partitioning of $PPTH_{2_T}$ between N^5-carbinolamine formation and the reduction of *m*-hydroxybenzaldehyde to *m*-hydroxybenzyl alcohol. That N^5-carbinolamine and N^5-imine are formed (Scheme V) was shown by $NaCNBH_3$ trapping of these species. The presence of intermediates formed by the addition of $PPTH_{2_T}$ to *m*-hydroxybenzaldehyde could also be established in reactions with molecular oxygen. The species PPT_{ox}^- and Fl_{ox} serve as catalysts in the formation of PPT_{ox}^- in the reaction of $PPTH_{2_T}$ with *m*-hydroxybenzaldehyde. The reduction of the aliphatic disulfides cystine and dithiodiglycolic acid by PPT^{2-} yields mercaptan and PPT_{ox}^- in 90–100% yields. These reactions are strongly catalyzed by traces of heavy metal ions. *N*-Alkylnicotinamides are also reduced by PPT^{2-}. The reactions of *N*-benzylnicotinamide and nicotinamide adenine dinucleotide with PPT^{2-} are first order in both reactants to ~8$t_{1/2}$ and give ~100% yields of PPT_{ox}^-. By employing *N*-benzylquinoline-3-carboxamide as the substrate it could be shown that the reduction with PPT^{2-} yields, in 100% of theory, both the nonhydratable *N*-benzyl-1,4-dihydroquinoline-3-carboxamide and PPT_{ox}^-. These various results are discussed as is the possibility that a pyrimido[4,5-*g*]pteridine could be recognized as a cofactor.

In the previous study (preceding paper in this issue)[1] there were described the synthesis, solution chemistry, and electrochemical potential determinations for 3,7,10-trimethyl-(3*H*,7*H*,9*H*,10*H*)-pyrimido[5,4-*g*]pteridine-2,4,6,8-tetrone (PPT_{ox}) and related compounds and their solvolysis products. The two-electron redox potential of the PPT_{ox}^-/PPT^{2-} couple at pH 7.0 is more negative than the corresponding redox potentials of flavins by 148 mV (Scheme I). The species PPT^{2-} is established, in the present study, to be an interesting reducing agent and a good 1,5-dihydroflavin mimic. Mechanistic deductions based on studies with PPT^{2-} as a reductant may be extended (with suitable care) to the same reactions run in the opposite direction with flavin as an oxidant.

Scheme I

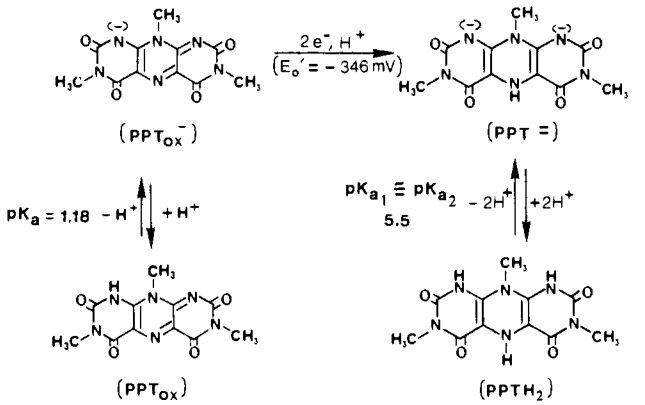

Flavoenzyme alcohol oxidases catalyze the oxidation of methanol and other primary alcohols to their respective aldehydes.[2] Flavins and many flavoenzymes are reduced by 1,4-dihydronicotinamide cofactors.[3] Enzyme-free flavins oxidize alkyl

(1) Skibo, E. B.; Bruice, T. C. *J. Am. Chem. Soc.* **1983**, *105*, preceding paper in this issue.

0002-7863/83/1505-3316$01.50/0

mercaptans to disulfides.[4] However, in the instance of glutathione reductase, lipoamide dehydrogenase, and possibly thioredoxin reductase, enzyme-bound 1,5-dihydroflavin cofactor reduces a cystine disulfide bond of the respective enzyme.[5,6]

There is provided, herein, a description of the findings when PPT^{2-} is employed as a reductant for aldehyde, *N*-alkylnicotinamide and alkyl disulfide moieties in aqueous solution. Since 1,5-dihydroflavins[7,8] and PPT^{2-} both reduce formaldehyde, a comparison of the kinetics of these reductions is presented. The notable similarities in these reactions include carbonyl group reduction in competition with formation of stable adducts and the breakdown of these adducts by a comproportionation mechanism. *m*-Hydroxybenzaldehyde is reduced by PPT^{2-} to *m*-cresol without the intermediacy of *m*-hydroxybenzyl alcohol. Adduct formation and comproportionation are also apparent in this system. A mechanism for this novel conversion is proposed.

Experimental Section

All kinetics were followed at 30 ± 0.2 °C with a Cary 118 or a Perkin-Elmer λ 3 spectrophotometer. Buffers and stock solutions were prepared with doubly distilled water. Buffer systems used were acetic acid/acetate (pH 4.5–5.5) and monobasic/dibasic phosphate (pH 6.0–8.0). The ionic strength was adjusted with KCl to 1.0. pH measurements were made with a Radiometer Model M26 pH meter equipped with a combined calomel glass electrode.

Materials. Formaldehyde was prepared according to the method of Gilman and Catlin[9] and assayed using the Hantzsh[10] reagent. *m*-Hydroxybenzaldehyde was recrystallized from water followed by two recrystallizations from hexane–ether. NAD^+, grade 3, was purchased from Sigma Chemical Co. *N*-Benzylnicotinamide bromide[11] and *N*-benzylquinoline-3-carboxamide bromide[12] were prepared according to literature procedures. Dithiodiglycolic acid, Aldrich, was purified by two recrystallizations from pentane/ether. L-Cystine was purchased from Schwarz Bioresearch.

3,7,10-Trimethyl-5-ethyl-(3*H*,5*H*,7*H*,10*H*)-pyrimido[5,4-*g*]pteridine-2,4,6,8-tetrone (N^5-EtPPT$_{ox}$). To a Parr bottle 0.5 g (1.7 mmol) of PPT_{ox}^-, 0.25 g of 10% palladium on charcoal, 250 mL of H_2O, 5.0 mL of acetaldehyde, and 25 mL of concentrated HCl were added. This mixture was hydrogenated under 35 psi H_2 for 2.5 days. After this time the catalyst was filtered off and the solids were washed several times with water to remove crystallized product. The filtrate was evaporated at room temperature in vacuo and the residue dissolved in methanol followed by addition of 5.0 g of 50–250-mesh silica gel. Evaporation gave the reaction product absorbed onto silica gel which was placed on a 150-mL 230–400-mesh silica gel column prepared with 10% methanol in chloroform. The product eluted off first with this solvent system leaving the starting material, PPT_{ox}^-, behind. Evaporation of the product fractions to 20 mL followed by dilution to 50 mL with diethyl ether resulted in crystallization of a red-orange solid: yield 0.059 g (10%); TLC on silica gel (10% methanol in chloroform) gave an R_f of 0.76. Anal. Calcd for $C_{13}H_{14}N_6O_4 \cdot 0.25H_2O$: C, 48.36; H, 4.52; N, 26.03. Found: C, 48.48; H, 4.67; N, 25.30. The theoretical and experimental nitrogen percentages deviate significantly, a common finding with the pteridine ring systems.[13] Storage as a solid at room temperature for 10 months resulted in ~50% conversion to PPT_{ox}^- (estimated by TLC and UV).

Kinetics of $PPTH_{2_T}$ Oxidation. A Thunberg cuvette was used to carry out photoreductions and to follow the rates of oxidation of $PPTH_{2_T}$ by substrates. The substrate, in the appropriate buffer, was added to the top port while to the bottom port there was added 0.4 mL of a solution 1.27×10^{-4} in PPT_{ox}^-, 0.1 mL of 0.1 M EDTA (at the pH of the buffer employed), and enough buffer such that the total volume of the top and bottom ports was 5.0 mL. The Thunberg was sealed (with Apiezon N grease), and the contents of upper and lower ports were deoxygenated by passing argon (filtered through an Oxiclear filter and then humidified) into the solution through thin Teflon tubes for 45 min. The tubes were removed and the Thunberg was closed. Photoreduction of the bottom port contents were carried out by using a water-cooled 300-W lamp or an Oriel arc lamp. Reduction time depended on pH with a time of 30 min needed for solutions at a pH of 4–5. At pH values of 6–8, photoreduction was complete in about 10 min. After equilibration at 30 ± 0.2 °C, the contents were mixed and the increase in absorbance was followed at 423 nm. The initial concentration of $PPTH_{2_T}$ on combining the contents of the ports at zero time was 1×10^{-5} M. Substrates were at least 20× as concentrated. All solutions used in the above experiment were at $\mu = 1.0$ with KCl.

Comproportionation and $NaCNBH_3$ trapping studies were carried out as described earlier for mechanistic studies of reactions of 1,5-dihydroflavin with carbonyl compounds.[7,8]

Heavy metal free, pH 7.00, 0.33 M phosphate buffer, 1.27×10^{-4} M PPT_{ox}^- in 1 M KCl, and pH 7.00, 0.1 M EDTA used in the study of disulfide reduction by $PPTH_{2_T}$ were prepared by dithiazone extraction. Solutions, ~100 mL, were extracted 5× with 50-mL portions of 0.01% dithiazone in methylene chloride followed by extraction 5× with 50-mL portions of methylene chloride. Removal of methylene chloride from the aqueous phase was carried out by purging with argon. All Thunberg cuvettes, pipet tips, and storage containers for solutions were soaked in 5% EDTA at pH 7 for 3 h followed by washing with copious amounts of distilled water.

Methods of Product Analysis. The percent yields of PPT_{ox}^- formed upon substrate reduction were determined spectrophotometrically at λ_{max} 432 nm ($\epsilon = 38\,100$ M cm^{-1}). Products formed by reduction of substrates were identified as follows.

(1) *m*-Cresol from PPT^{2-} Reduction of *m*-Hydroxybenzaldehyde. A solution of 0.25 g (2.07 mmol) of *m*-yydroxybenzaldehyde in 50 mL of pH 7.00 phosphate buffer was deoxygenated with N_2 for 3 h. After transfer into a N_2 glovebox 0.6 g of $PPTH_2$ (2.04 mmol) was added and the reaction stirred for 4 weeks at room temperature. The reaction was removed from the glovebox and extracted 5× with 15-mL portions of chloroform. The extracts were dried over $MgSO_4$, filtered, and diluted to 100 mL in a volumetric flask. A 10-mL aliquot was removed and added to a volumetric flask containing 11.82 mg of hexaethylbenzene. A Varian Model 3700 gas chromatograph equipped with a 6-ft OV-17 column utilizing a flame ionization detector was used to determine peak areas for unreacted *m*-hydroxybenzaldehyde, *m*-cresol, and hexaethylbenzene. A 10 mL chloroform solution of authentic *m*-hydroxybenzaldehyde (11.09 mg) and *m*-cresol (24.61 mg) was prepared with 11.82 mg of hexaethylbenzene added as an internal standard. Comparison of the peak areas for the components in the standard and those for the solution of reaction products allowed determination of the total amount of *m*-hydroxybenzaldehyde (154 mg, 61%) and *m*-cresol (67.3 mg, 30%) formed in the reaction.

For the identification of *m*-cresol as a reduction product the remaining chloroform extracts (90 mL) were concentrated to 2 mL and applied to two preparative silica gel plates (Analtech silica gel GF, 1000 μm). The plates were developed twice with 5% methanol in chloroform. The product band, moving slightly faster than that of the aldehyde, was scraped off and extracted with methanol. Removal of silica gel by filtration and concentration in vacuo yielded an oil pure by GC. The IR spectrum, obtained from a thin film between NaCl disks, was identical with that of authentic *m*-cresol. The crystalline derivative, *m*-tolyl *N*-phenylcarbamate, was prepared by treatment of the above product with phenyl isocyanate in petroleum ether. The melting point was 117–118 °C (lit. mp 121–122 °C[14]) and mixture melting point was 123–124 °C.

(2) Nicotinamide Reduction Product Studies. Reduction of 1.5 g (5.3 mmol) of *N*-benzylnicotinamide bromide by 1.7 g (5.8 mmol) of $PPTH_2$ was carried out in pH 7.00 phosphate buffer under anaerobic conditions.

(2) Mincey, T.; Tayrien, G.; Mildvan, A. S.; Abeles, R. H. *Proc. Natl. Acad. Sci. U.S.A.* **1980**, *77*, 7099. Patel, R. N.; Hou, C. T.; Laskni, A. I.; Derelanko, P. *Arch. Biochem. Biophys.* **1981**, *210* (2), 481. Geissler, J.; Hemmerich, P. *FEBS Lett.* **1981**, *126*, 152.

(3) Hemmerich, P.; Nagelschneider, G.; Veeger, C. *FEBS Lett.* **1970**, *8*, 69.

(4) Yokoe, I.; Bruice, T. C. *J. Am. Chem. Soc.* **1975**, *97*, 450. Loechler, E. L.; Hollacher, T. C. *Ibid.* **1975**, *97*, 3235. Sayer, J. M.; Coulou, P.; Huff, J.; Faucher, J.; Belanger, R.; White, E. J. *Ibid.* **1979**, *101*, 1890. Loechler, E. L.; Hollacher, T. C. *Ibid.* **1980**, *102*, 7312, 7322, 7328.

(5) Anscott, L. D.; Thorpe, C.; Williams, C. H. Jr. *Biochemistry* **1981**, *20*, 1513.

(6) Williams, C. H. Jr. *Enzymes, 3rd Ed.* **1976**, *13*, 89.

(7) Williams, R. F.; Bruice, T. C. *J. Am. Chem. Soc.* **1976**, *98*, 7752.

(8) Williams, R. F.; Shinkai, S. S.; Bruice, T. C. *Ibid.* **1977**, *99*, 921.

(9) Gilman, H.; Catlin, W. E. "Organic Synthesis", Wiley: New York, 1941; Collect. Vol. 1, p 188.

(10) Nash, T. *Biochem. J.* **1953**, *55*, 416.

(11) Harrer, P.; Stare, F. J. *Helv. Chim. Acta* **1937**, *20*, 418.

(12) Shinkai, S.; Hamada, H.; Kusano, Y.; Manabe, O. *J. Chem. Soc., Perkin Trans. 2* **1979**, 699.

(13) Albert, A. "Chemistry and Biology of Pteridines"; Pfleiderer, W., ed.; Walter de Druyter: New York and Berlin, 1975; pp 1–26.

(14) Huntress, E. H.; Mulliken, S. P. "Identification of Pure Organic Compounds"; Wiley: New York, 1971; p 258.

(15) Anderson, B. M.; Reynolds, M. L.; Anderson, C. D. *Arch. Biochem. Biophys.* **1965**, *110*, 577. Stock, A.; Sann, E.; Pfleiderer, G. *Justus Liebigs Ann. Chem.* **1961**, *647*, 188. Burton, R. M.; Kaplan, N. O. *Arch. Biochem. Biophys.* **1963**, *101*, 150. Johnson, C. C.; Gardner, J. L.; Suelter, C. H.; Metzler, D. E. *Biochemistry* **1963**, *2*, 689. Oppenheimer, N. J.; Kaplan, N. O. *Biochemistry* **1974**, *13*, 4675.

Scheme II

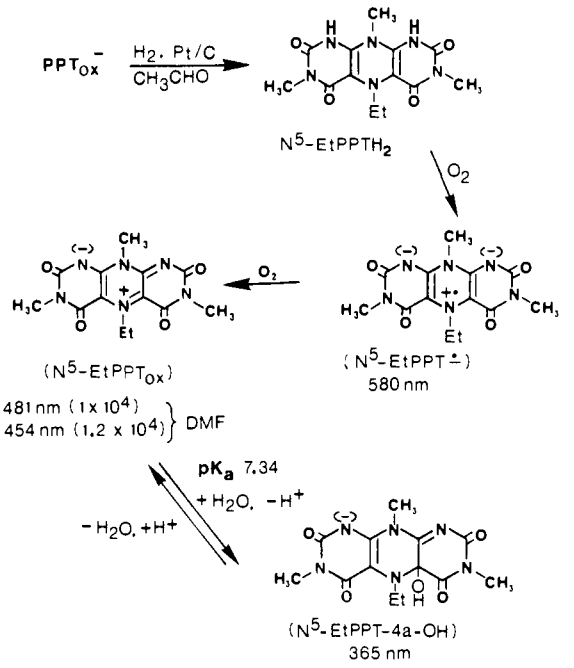

After a 2-day reaction time the reaction mixture was exposed to the air and extracted 3× with 50 mL of ethyl acetate. Drying of the extracts over $MgSO_4$, filtration, and concentration in vacuo yielded 0.76 g (57%) of the hydrate of *N*-benzyl-1,4-dihydronicotinamide. Spectrophotometric data, λ_{max} 290 nm, and NMR are consistent with this structure assignment. The hydrolytic lability of 1,4-dihydropyridine compounds has been documented.[14]

(3) *N*-Benzylquinoline-3-carboxamide Reduction Product. A solution of *N*-benzylquinoline-3-carboxamide (100 mg, 0.3 mmol) in 10 mL of pH 7.00, phosphate buffer was deoxygenated for 3 h with argon. After transfer into a N_2 glovebox, 100 mg (0.34 mmol) of $PPTH_2$ was added and stirring carried out for 12 h. The reaction mixture was removed from the glovebox and extracted 3× with 50 mL of chloroform. Extracts were dried over $MgSO_4$, filtered, and concentrated in vacuo to a colorless solid identified as *N*-benzyl-1,4-dihydroquinoline, 85 mg (~100%). Identity was confirmed by TLC (R_f 0.73 on silica gel with 30% methanol in chloroform) and NMR. Recrystallization from water–methanol (1:3) gave colorless needles, mp 152–153 °C (lit. mp 155 °C).[12]

(4) Disulfide Reduction Product assays were carried out spectrophotometrically with 5,5′-dithiobis(2-nitrobenzoic acid) at pH 8.00 under anaerobic conditions.[16] To the bottom port of a three-port Thunberg 4.0 mL of 0.33 M, pH 8.00, phosphate buffer, 0.4 mL of 1.27×10^{-4} M PPT_{ox}^-, and 0.1 mL of 0.1 M EDTA were added. In one top port 0.1 mL of 0.01 M 5,5′-dithiobis(2-nitrobenzoic acid) dissolved in 0.33 M phosphate buffer (pH 7.0) was added. To the other port 0.5 mL of ~0.02 M disulfide (dithiodiglycolic acid or cystine) was added. Degassing and photoreduction of PPT_{ox}^- were carried out as described above. Combination of the port containing disulfide with the bottom port resulted in PPT_{ox}^- formation (423 nm). At completion (90–100%) the absorbance at 412 nm was measured and the contents of the third port were added. Measurement of the concentration of 5-mercapto-2-nitrobenzoic acid formed from thiol was carried out at λ_{max} 412 nm (ϵ = 14 400 at pH 8.00).

Results

Reductive alkylation of PPT_{ox}^- with acetaldehyde (Scheme II) provides the N^5-ethyl derivative of $PPTH_2$ [3,7,10-trimethyl-5-ethyl-(1*H*,3*H*,7*H*,9*H*,10*H*)-pyrimido[5,4-*g*]pteridine-2,4,6,8-tetrone or N^5-$EtPPTH_2$]. Our objectives in preparing N^5-$EtPPTH_2$ have been (i) to compare the chemistry of the N^5-Et flavin and appropriate N^5-ethylpyrimido[5,4-*g*]pteridine and (ii) to provide an analogue of N^5-alkyl-$PPTH_2$ formed by reductive trapping of N^5-carbinolamine and N^5-imine species present during reaction of PPT^{2-} with aldehydes (vide infra).

In Aqueous Solution N^5-$EtPPTH_2$ Reacts with O_2 To Yield the Iminium Radical, N^5-$EtPPT^{-}$·. As in the case of flavins, N^5-alkylation greatly stabilizes the radical species. The mixing of solutions of PPT_{ox}^- and PPT^{2-} does not give rise to appreciable radical formation between pH 7 and pH 11. Much the same is true for the comproportionation of Fl_{ox} and FlH^-.[18]

Further O_2 Oxidation of N^5-$EtPP^{-}$· Yields the Quinoid Species N^5-$EtPPT_{ox}$ (Scheme II). The spectrum of N^5-$EtPPt^{-}$· and N^5-$EtPPT_{ox}$ may be compared to those of the corresponding flavin species, N^5-EtFl·[18] and N^5-$EtFl_{ox}^+$,[19] eq 1.

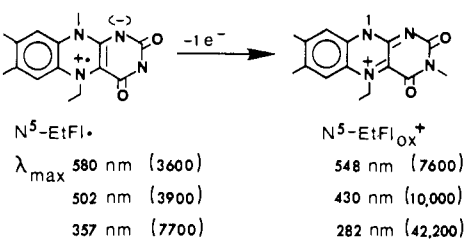

(1)

The pseudobase N^5-EtPPT-4a-OH is obtained on addition of HO^- to the 4a-position of N^5-$EtPPT_{ox}$. The spectrum of N^5-EtPPT-4a-OH resembles that of the pseudobase of N^5-$EtFl_{ox}^+$ (compare eq 2 and Scheme II). The pK_a for pseudobase formation with N^5-$EtPPT_{ox}$ (7.34) exceeds that for the formation of the pseudobase of N^5-$EtFl_{ox}^+$ (pK_a 4.0)[19] by ~3 pH units. This is due to the greater electron density of N^5-$EtPPT_{ox}$ as compared to that of N^5-$EtFl_{ox}^+$.

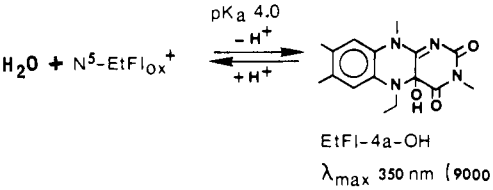

(2)

The formation of N^5-$MePPTH_2$ by $NaCNBH_3$ reduction of PPT_{ox}^- in the presence of formaldehyde has been investigated. In the instance of the 1,5-dihydroflavin reactions with carbonyl compounds, the presence of the N^5-carbinolamine or N^5-imine could be determined quantitatively by trapping with $NaCNBH_3$ and oxygenation of the solution to generate the N^5-alkylflavin radical. This procedure allowed the quantitative (spectral) determination of the concentration of N^5-carbinolamine and N^5-imine adducts.[7,8] On the basis of this experience it might be supposed that the N^5-carbinolamine and N^5-imine formed from $PPTH_2$ and CH_2O (vide infra) could perhaps be trapped quantitatively with $NaCNBH_3$ and converted by O_2 oxidation to N^5-$MePPT_{ox}$ and N^5-MePPT·. Of concern is the stability of these N^5-methyl derivatives and the specificity of this analytical procedure.

Since N^5-$EtPPT_{ox}$ possesses a pseudobase pK_a of 7.34, studies were carried out at pH 5.5 in 0.4 M acetate buffer. A 8.76×10^{-4} M solution of N^5-$EtPPT_{ox}$ exhibited little change in absorbance (λ_{max} 481 nm) over a period of 1 h at this pH. Oxidized flavin (Fl_{ox}) is not reduced by $NaCNBH_3$ in aqueous solution in the presence or absence of CH_2O under anaerobic conditions. The oxidized pyrimidopteridine, PPT_{ox}^- (1×10^{-5} M), is also not reduced in aqueous solution in the presence of excess $NaCNBH_3$ at pH 5.5. In the presence of 0.06 M CH_2O, however, PPT_{ox}^- is completely reduced by $NaCNBH_3$ in ~200 s. Addition of O_2 at this time provided N^5-$MePPT_{ox}$ and N^5-$MePPT^{-}$· (Scheme III). Structural assignment was based on spectral similarity to the N^5-Et analogues (Scheme II). Since PPT_{ox}^- cannot yield an N^5-carbinolamine with CH_2O and is itself not reduced by $NaCNBH_3$, it is required that PPT_{ox}^- react with CH_2O to provide an adduct

(16) Bruice, P. Y.; Wilson, S. C.; Bruice, T. C. *Biochemistry* **1978**, *17*, 1662.
(17) Kemal, C.; Bruice, T. C. *Proc. Natl. Acad. Sci. U.S.A.* **1976**, *73*, 995. Ball, S.; Bruice, T. C. *J. Am. Chem. Soc.* **1981**, *103*, 5494.
(18) Muller, F.; Brustlein, M.; Hemmerich, P.; Massey, V.; Walker, W. H. *Eur. J. Biochem.* **1972**, *25*, 573.
(19) Gisla, S.; Hartmann, U.; Hemmerich, P.; Muller, F. *Justus Liebigs Ann. Chem.* **1973**, 1388.

Scheme III

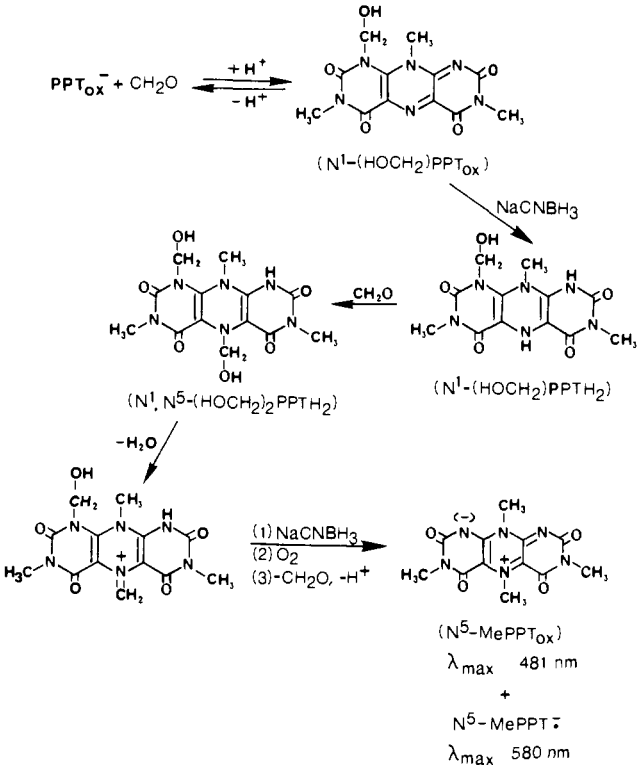

which is reducible by $NaCNBH_3$ and that this reduced adduct can then yield an N^5-carbinolamine with CH_2O. The reactions of Scheme III are suggested.

The N^1-carbinolamine of PPT_{ox}^-, N^1-$(HOCH_2)PPT_{ox}$, is expected to exhibit the redox properties of N^1-$MePPT_{ox}$ ($E^{\circ\prime} = -147$ mV vs. $E^{\circ\prime} = -346$ mV for PPT_{ox}^-).[1] Consistent with this is the finding that N^1-$MePPT_{ox}$ is reduced by $NaCNBH_3$ and reappears on addition of oxygen, eq 3. A detailed kinetic study of this

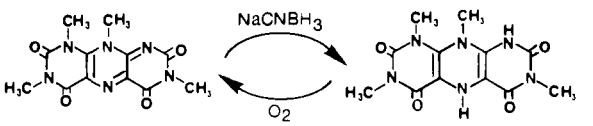

(3)

reaction was hindered by the solvolysis of N^1-$MePPT_{ox}$ (see preceding paper in this issue).

These results bear on the use of the analytical procedure wherein $NaCNBH_3$ reduction is employed to show the presence of N^5-carbinolamine and N^5-imine in the reaction of $PPTH_{2_T}$ with CH_2O, eq 4 (vide infra). Since PPT_{ox}^-, produced as a product of aldehyde reduction, can itself yield N^5-$MePPT_{ox}$ in the presence of aldehyde and $NaCNBH_3$ (Scheme III), the $NaCNBH_3$ trapping procedure is not uniquely specific for N^5-carbinolamines and imines formed as intermediates in the reaction of $PPTH_2$ with CH_2O.

The kinetics of the reaction of formaldehyde with $PPTH_2$ were studied in aqueous solution under anaerobic conditions between pH 4.0 and pH 7.6 by using the pseudo-first-order conditions of $[CH_2O_T] = 1 \times 10^{-3}$–$4 \times 10^{-2}$ M $\gg [PPTH_{2_T}] = 1 \times 10^{-5}$ M (where $[PPTH_{2_T}] = [PPTH_2] + [PPTH^-] + [PPT^{2-}]$ and $[CH_2O_T] = [CH_2O] +$ [hydrated species][20]). The kinetics for reaction proved to be multiphasic. An initial burst of formation of PPT_{ox}^- (423 nm) was followed by a much slower formation of PPT_{ox}^-. The multiphasic character as well as the rate constants were not affected by a 10-fold change in [buffer] at pH 6.67 (phosphate, 0.30–0.03 M) and at pH 4.00 (acetate, 0.35–0.03 M). The formation of PPT_{ox}^- with time was fit by either of two computer programs. The first program assumed that PPT_{ox}^- is formed via two consecutive pseudo-first-order rate processes with the rate

(20) Zavitsas, A. A.; Coffiner, M.; Wiseman, T.; Zavitsas, L. R. *J. Phys. Chem.* **1970**, *74*, 2746.

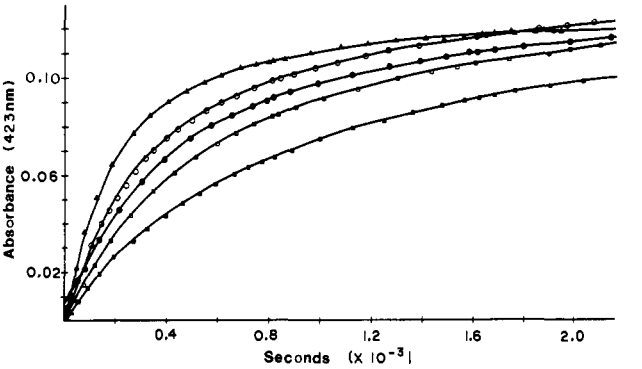

Figure 1. Absorbance (423 nm) vs. time plots for the reaction of $PPTH_{2_T}$ (1×10^{-5} M) with CH_2O in pH 7.00 buffer (0.33 M phosphate, $\mu = 1.0$ KCl) at 30 °C under anaerobic conditions. $[CH_2O]$: (▲) 0.0012 M; (○) 0.0018 M; (●) 0.0024 M; (□) 0.003 M; (■) 0.006 M.

Table I. Percent Total PPT_{ox}^- Formed during the Initial Burst at Various pHs[a]

pH	% total PPT_{ox}^-	pH	% total PPT_{ox}^-
4.00	23	6.25	27
4.25	20	6.50	27
4.50	27	6.75	31
4.75	18	7.00	26
5.00	28	7.45	25
6.00	28	7.60	24

[a] Each percent is an average of values obtained for a series of $[CH_2O]$ at constant pH.

of the first reaction (the burst) exceeding that of the second reaction. Since the second process was very slow, it became convenient to follow it to only ~50% completion. In this instance the formation of PPT_{ox}^- with time was fit to a program for sequential first- and zero-order reactions because plots of appearance of products in first-order reactions are linear with time to ca. 40% completion of reaction. Examples of data points for A_{423} vs. time are shown in Figure 1 for the reaction of $PPTH_{2_T}$ with CH_2O_T at pH 7.0. When reactions were followed for several days, so that the second phase had continued to completion, it was found that formation of PPT_{ox}^- ceased at 33%, based upon initial $[PPTH_{2_T}]$ regardless of $[CH_2O]$ and pH. The second phase of the reaction accounted for only ~8% conversion of $PPTH_{2_T}$ to PPT_{ox}^-, while the initial first-order component accounted for 25% conversion of $PPTH_{2_T}$ to PPT_{ox}^- regardless of the formaldehyde concentration and pH (Table I). In addition, the pseudo-first-order rate constants for the first phase of reaction (initial burst in PPT_{ox}^- formation) exhibited saturation in formaldehyde, as shown in Figure 2. The simplest empirical equation which fits the points of Figure 2 is that of eq 4. The slopes of plots of A_{423} for the

$$k_{obsd} = \bar{K}[CH_2O_T]/(\bar{K} + [CH_2O_T]) \quad (4)$$

second phase of reaction (zero-order component) vs. time varied from 1×10^{-5} to 3×10^{-5} OD unit/s, having no significant dependence upon pH or concentration of formaldehyde. The rather random values of the initial rates for the second phase reflect the errors which come about by approximation of the initial part of a first-order reaction as zero order.

The kinetic order in $[CH_2O_T]$ for the rate-determining step in the formation of $PPTH_{2_T}$ adduct(s) must be the same as that for reduction of CH_2O by $PPTH_2$. This is shown by the observation that the ratio of PPT_{ox}^- and adduct formed in the initial reaction is independent of $[CH_2O_T]$. Since the reduction of CH_2O by $PPTH_{2_T}$ is first order in $[CH_2O_T]$, below saturation in this species, the formation of the $PPTH_{2_T}$–formaldehyde adduct(s) must also be first order in $[CH_2O_T]$. In addition, the rate for the formation of adduct(s) must also exhibit saturation in $[CH_2O_T]$ and the same pH dependence as does PPT_{ox}^- formation.

After termination of PPT_{ox}^- formation, addition of O_2 resulted in the slow formation of additional PPT_{ox}^- to 100% yield based on initial $[PPTH_{2_T}]$. Typical rate constants for the O_2-mediated

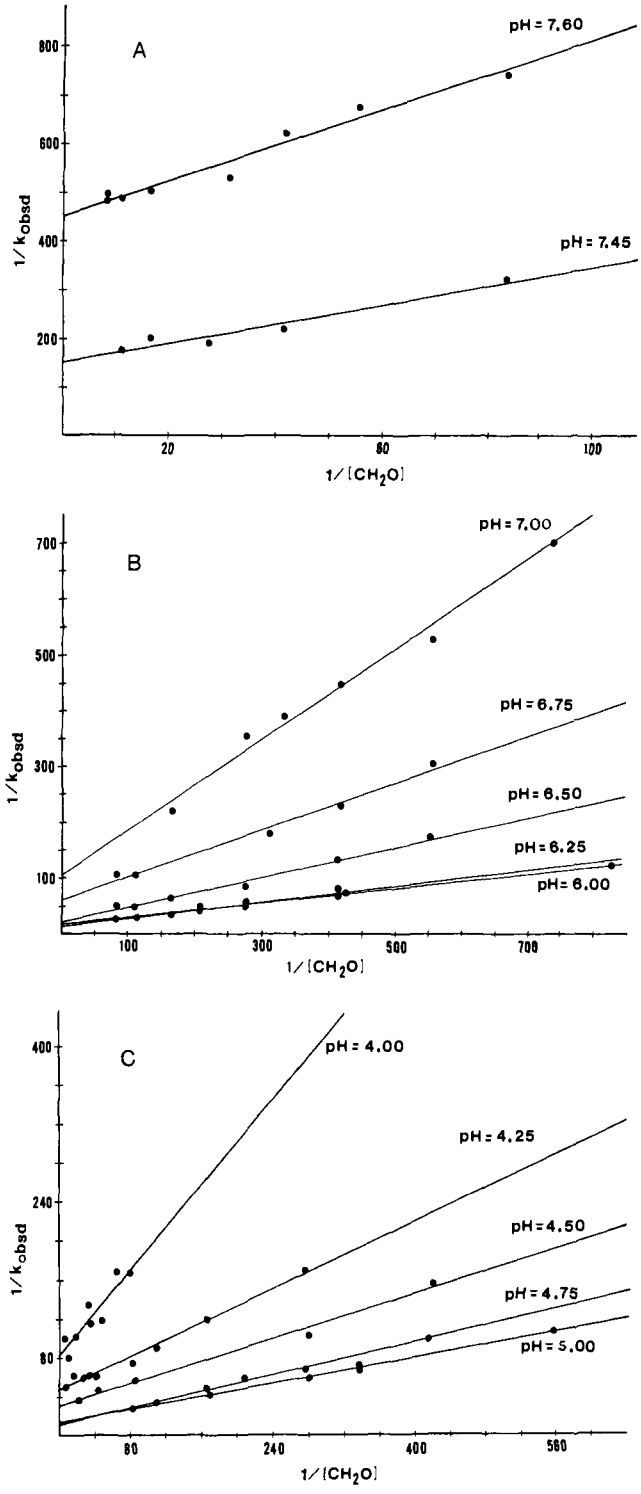

Figure 2. Reciprocal plots of first order component (s^{-1}) dependence on $[CH_2O]$ for reduction by 1×10^{-5} M $PPTH_{2T}$ at 30 °C. (A) 0.33 M phosphate buffer, μ = 1.0 KCl. (B) 0.33 M phosphate buffer, μ = 1.0 KCl. (C) 0.4 M acetate buffer, μ = 1.0 KCl.

formation of PPT_{ox}^- ($[CH_2O_T] = 1.3 \times 10^{-2}$ M) are 4.83×10^{-4} s^{-1} (pH 4.0) and 2.1×10^{-3} s^{-1} (pH 5.0). At higher pH (>7.0) O_2 oxidation to yield PPT_{ox}^- is very rapid, occurring in the stopped-flow time range. The approximately 10-fold increase in rate on going from pH 4.0 to pH 5.0 is consistent with this observation. These rate constants are far smaller than expected for O_2 oxidation of $PPTH_{2T}$ since a $PPTH_{2T}$ solution at these pH values immediately oxidizes on contact with air. Thus, the $PPTH_{2T}$–formaldehyde adducts possess a much higher redox potential than $PPTH_{2T}$, accounting for the termination of formaldehyde reduction.

The findings which we have enumerated to this point may then be summarized as follows: (1) under the pseudo-first-order conditions of $[CH_2O_T] \gg [PPTH_{2T}]$ there is formed, in the absence of O_2, a 33% yield of PPT_{ox}^-; (2) the appearance of PPT_{ox}^- with time is biphasic, consisting of an initial first-order burst followed by a slower first-order reaction also; (3) the second phase of the reaction is not affected by $[CH_2O_T]$ or pH, while the rate constant for the first-order burst is both pH and $[CH_2O_T]$ dependent, exhibiting saturation at high $[CH_2O_T]$; (4) since only 33% $PPTH_{2T}$ is converted to PPT_{ox}^-, the remainder of $PPTH_{2T}$ must be combined with formaldehyde [as a high redox potential adduct(s) which does (do) not reduce CH_2O] and in this form is slowly oxidized to PPT_{ox}^- in the presence of O_2.

At any constant value of pH, the sequence of events in eq 5

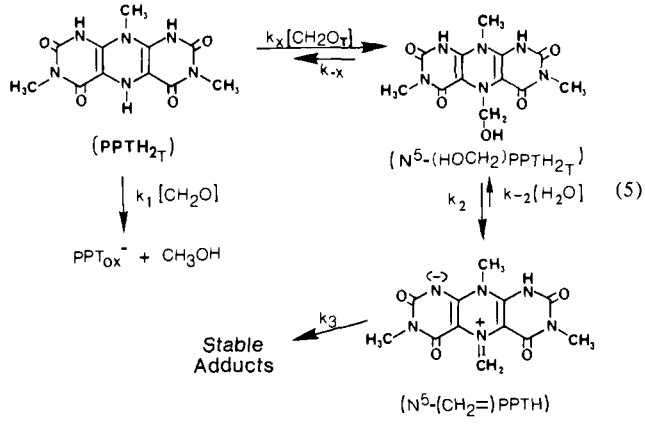

(5)

may be used to explain these kinetic observations. Drawing upon the analogous reactions of 1,5-dihydroflavin with pyruvate[7] and formaldehyde[8] as well as the methodology used in the synthesis of N^5-EtPPT_{ox} (loc. cit.), one may suppose that $PPTH_{2T}$ is in equilibrium with its N^5-carbinolamine [N^5-$(HOCH_2)PPTH_{2T}$]. Elimination of water from the carbinolamine can then occur (k_2, eq 5) to form the imine, N^5-$(CH_2{=})PPTH_{2T}$. Competing with this process is the direct reduction of formaldehyde by $PPTH_{2T}$ (k_1, eq 5). Thus, during the initial burst both PPT_{ox}^- and N^5-$(CH_2{=})PPTH_{2T}$ are formed and the rate of the partitioning of $PPTH_{2T}$ exhibits saturation in formaldehyde. That PPT_{ox}^- is formed in only 23% yield during the initial burst may be a consequence of the relative rates of formaldehyde reduction vs. imine formation, $k_1/k_2 = 0.25$ (if $k_2 > k_{-x}$, eq 5).

The relatively slow hydration of the N^5-imine to yield N^5-carbinolamine, as implied in eq 5, is based on the presumed stabilization of N^5-imine in the ionized form by either oxazolidine ring formation, structures A–C, eq 6, or by steric hindrance by the carbonyl functions at positions 4 and 6.

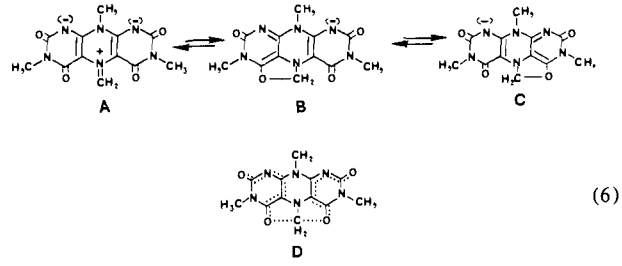

(6)

Examination of Stuart-Briegleb space-filling models suggests that the resonantly stabilized species D is not unreasonable. Thus, the slow phase of PPT_{ox}^- formation, shown to be independent of $[CH_2O_T]$, could be accounted for by a rate-determining hydration of the N^5-imine (k_{-2} in eq 5). Assumption of PPT_{ox}^- formation from the N^5-imine, where [$N^5(HOCH_2)PPTH_{2T}$] and [$PPTH_{2T}$] are at steady state, leads to an expression without $[CH_2O_T]$ terms, eq 7. Since this slow phase does not proceed to completion, a

$$k_{obsd} = \frac{k_1 k_{-2} k_{-x}}{k_{-x} k_1 + k_2(k_1 + k_x)} [N^5\text{-}(CH_2{=})PPTH_{2T}] \quad (7)$$

Scheme IV

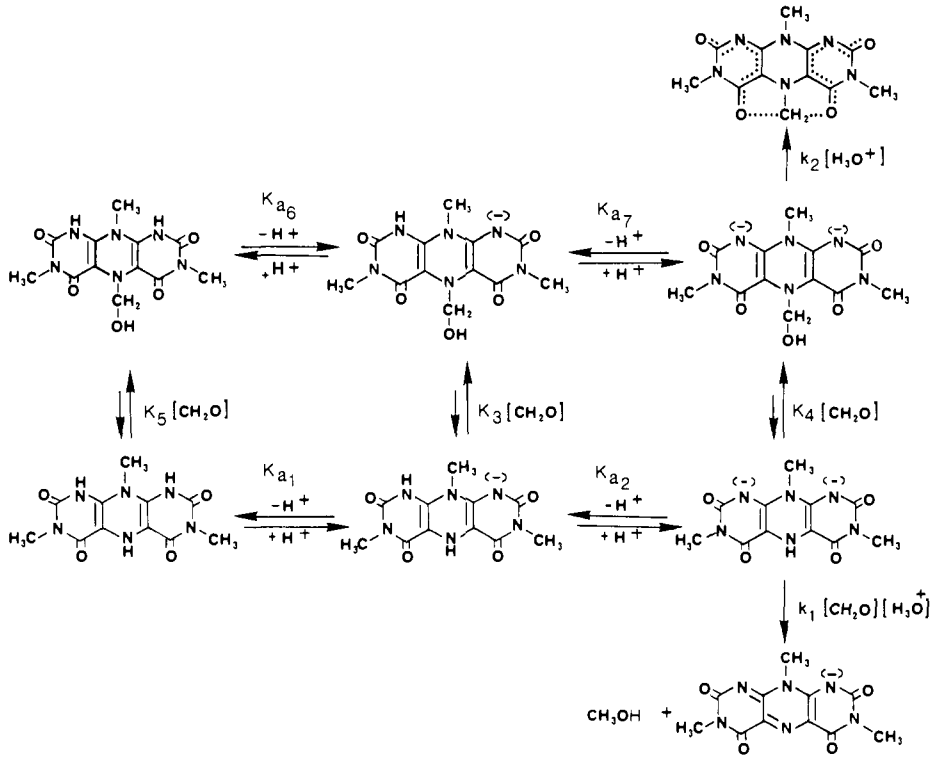

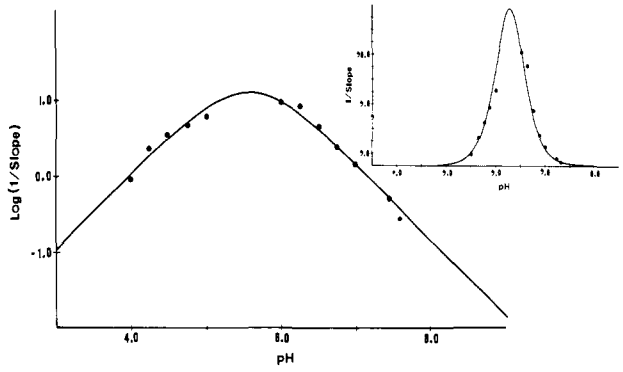

Figure 3. Plot of log (1/slope) obtained from reciprocal plots of Figure 2 vs. pH for the first-order component of reaction of $PPTH_{2_T}$ (1×10^{-5} M) with formaldehyde. The theoretical line connecting the experimental points was generated with eq 6; constants were determined by iteration. The inset is a plot of 1/slope vs. pH with the solid line generated from the constants determined above.

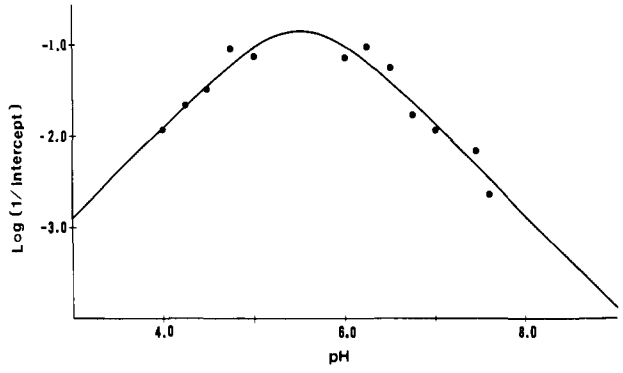

Figure 4. Plot of log (1/intercept) obtained from reciprocal plots of Figure 2 vs. pH for the first-order component of reaction of $PPTH_{2_T}$ (1×10^{-5} M) with formaldehyde. Theoretical line connecting the experimental points was generated by eq 6, constants were determined by iteration.

competing rate process (k_3 in eq 5) leading to formation of "stable adducts" from the N^5-imine must occur. The chemistry of this termination is discussed (vide infra).

The pH dependence for the initial first-order burst of PPT_{ox}^- and N^5-imine formation on reaction of formaldehyde with $PPTH_{2_T}$ will now be discussed. In the reaction sequence described by eq 5 the dependence of k_{obsd} for the burst reaction upon $[CH_2O_T]$ is given in eq 4. Plotting $1/k_{obsd}$ vs. $1/[CH_2O]$ at a constant value of pH, as in Figure 2, gives $1/\bar{K}$ as the intercept and $1/\bar{K}$ as slope. Plots of log (slope^{-1}) and log (intercept^{-1}) vs. pH provided "bell-shaped" profiles with maxima at pH 5.5 (Figures 3 and 4, respectively). The points of these plots are experimental and the lines were generated by use of the empirical equation

$$k_{obsd} = \frac{\bar{K}_1 a_H}{\bar{K}_2 + \bar{K}_3 a_H + a_H^2} \quad (8)$$

where $\bar{K}_1$, $\bar{K}_2$, and $\bar{K}_3$ are constants determined by iteration. This pH dependence for the initial first-order burst of PPT_{ox}^- formation may be quantitatively expressed by considering all the ionic forms of the species in eq 5 as depicted in Scheme IV. Assumption of

Table II. Rate and Equilibrium Constants for the Reaction of Formaldehyde with $PPTH_{2_T}$ (30 °C, H_2O Solvent, $\mu = 1.0$)

$k_1 + k_2K_4 = 1.44 \times 10^7$ M^{-2} s^{-1}
$k_1/k_2K_4 = 0.3$ (from initial burst partitioning of $PPTH_{2_T}$)
$k_1 = 3.3 \times 10^6$ M^{-2} s^{-1}
$k_2K_4 = 1.1 \times 10^7$ M^{-2} s^{-1}; $k_2 = 1.0 \times 10^5$ M^{-1} s^{-1}
$pK_{a_1} = 5.52$
$pK_{a_2} = 5.60$
$pK_{a_6} = 5.57$
$pK_{a_7} = 5.44$
$K_3 = 74$ M^{-1}
$K_4 = 107$ M^{-1}
$K_5 = 84$ M^{-1}

material balance for all species in equilibrium provides eq 9 for the first-order burst in PPT_{ox}^- and N^5-adduct formation.

$$k_{obsd} = (k_1a_H + k_2K_4a_H)K_{a_1}K_{a_2}[CH_2O]/[[CH_2O] \times (K_{a_2}K_{a_1}K_4 + K_3K_{a_1}a_H + K_5a_H^2) + a_H^2 + K_{a_1}a_H + K_{a_1}K_{a_2}] \quad (9)$$

Taking the inverse of eq 9 provides eq 10 which has the form of the inverse of eq 4. The terms slope^{-1} and intercept^{-1} of eq 10

$$\frac{1}{k_{obsd}[PPT_{ox}]} = \frac{1}{[CH_2O]}\left(\frac{a_H^2 + K_{a_1}a_H + K_{a_1}K_{a_2}}{(k_1a_H + k_2K_4a_H)K_{a_1}K_{a_2}}\right) + \frac{K_{a_2}K_{a_1}K_4 + K_3K_{a_1}a_H + K_5a_H^2}{(k_1a_H + k_2K_4a_H)K_{a_1}K_{a_2}} \quad (10)$$

both follow the empirical relationship for a bell-shaped log k_{obsd} vs. pH profile, eq 8, as required experimentally (Figures 3 and 4). From the constants of equation 8, determined by iteration (loc. cit.), and eq 10 there were obtained the individual rate and equilibrium constants of Scheme IV (Table II).

The properties of the stable adducts which terminate formation of PPT_{ox}^- when $PPTH_{2_T}$ and CH_2O_T are combined were investigated. A solution of adduct(s), without PPT_{ox}^-, was prepared by the photocatalytic reduction of PPT_{ox}^- (1×10^{-5} M) by EDTA (2×10^{-3} M) in an argon scrubbed solution containing formaldehyde (0.06 M) at pH 7.00 (0.33 M phosphate buffer). As PPT_{ox}^- is photoreduced to $PPTH_2$ the latter reacts with CH_2O_T. All PPT_{ox}^- formed on reaction of $PPTH_{2_T}$ with formaldehyde (initial burst reaction) is photoreduced so that all product PPT_{ox}^- ends up as $PPTH_2$ adducts of formaldehyde at termination of the photolysis. The UV–vis spectrum of the contents of the resulting solution closely resembles that of a solution 1×10^{-5} M in PPT^{2-} at pH 7.0 and on addition of O_2, PPT_{ox}^- is quantitatively re-formed (Figure 5). The close similarity in UV–vis spectra of PPT^{2-} and formaldehyde adduct(s) indicates the two to be isoelectronic. This experiment supports the contention that N^5-(CH_2=)PPTH is not one of the stable adducts of eq 5. When PPT_{ox}^- was photoreduced with EDTA in the presence of CH_2O_T (pH 5.5 with 0.4 M acetate buffer) and ~20 mg of $NaCNBH_3$ added followed in 3 min by bubbling O_2 into the solution, there could be observed (spectrally) the species N^5-$MePPT_{ox}$ and N^5-$MePPT^{\cdot}$. Since PPT_{ox}^- is absent from the solution at the time of $NaCNBH_3$ addition, it may be concluded that N^5-$MePPT_{ox}$ and N^5-$MePPT^{\cdot}$ formation does not occur by the mechanism of Scheme III. Thus, the stable adduct(s) which terminate(s) PPT_{ox}^- formation in the reaction of $PPTH_2$ and CH_2O_T are N^5-adducts of $PPTH_2$ which are reducible by $NaCNBH_3$ to N^5-$MePPTH_T$.

It is known that N^5-EtFlH does not reduce CH_2O due to the increase in redox potential which accompanies N^5-alkylation of reduced flavin. In separate experiments, carried out under anaerobic conditions, it was found that N^5-$EtPPTH_{2_T}$ and N^1-$MePPTH_{2_T}$ (both at 8.76×10^{-4} M in 0.4 M acetate buffer at pH 5.5) do not reduce formaldehyde (0.06 M). The compounds N^5-$EtPPTH_{2_T}$ and N^1-$MePPTH_2$ may be considered as analogues of the N^5- and N^1-formaldehyde adducts of $PPTH_2$. These results are consistent with the high redox potential (compared to that of $PPTH_2$) of the N^1-$MePPT_{ox}/N^1$-MePPTH couple of $E^{\circ\prime}$ = −147 mV and the expected high potential of the N^5-$EtPPT_{ox}/N^5$-$EtPPTH_{2_T}$ system.[21] Thus, the inability of the stable adducts of CH_2O and $PPTH_2$ to reduce CH_2O may be N^1-$MePPT_{ox}/N^1$-$MePPTH_{2_T}$ on the basis of the formation of N^1- and N^5-adducts. The reaction of oxygen with N^5-$EtPPTH_2$ and N^1-$MePPTH_{2_T}$ is, however, rapid, yielding N^5-$EtPPT^{\cdot}$ and N^1-$MePPT_{ox}$, respectively, whereas the reaction of oxygen with the "stable" (eq 5) formaldehyde adduct(s) of $PPTH_2$ consists of a slow first-order formation of PPT_{ox}^-. Presumably the slower reacting adduct possesses a redox potential more positive than those of the N^1- and N^5-alkyl-PPT systems. A good candidate for the unreactive $PPTH_2$ adduct(s) with formaldehyde would be an N^1,N^5-disubstituted $PPTH_2$ or N^1,N^5,N^9-trisubstituted $PPTH_2$. N^1,N^5-Dialkylflavins possess very positive potentials compared to flavins.[21]

In light of these observations a number of product structures could be suggested to account for the slow reaction of the final adducts formed on reaction of $PPTH_2$ and CH_2O. The termination of formation of PPT_{ox}^- from adducts may be due to dimerization of the N^5-imine (structure E) or the reaction of the N^5-

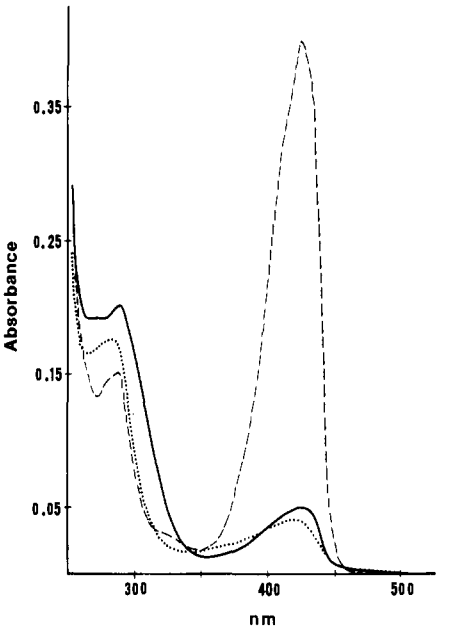

Figure 5. Spectra of 1×10^{-5} M PPT_{ox}^- (---), 1×10^{-5} M PPT^{2-} (—), and formaldehyde adduct (···) in 0.33 M, pH 7.00, phosphate.

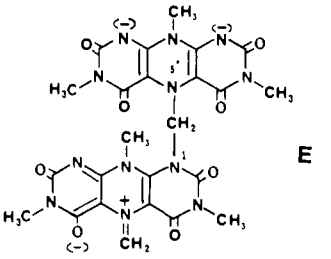
E

could lead to polymer. This process would be first order in formaldehyde as required experimentally. Also likely is the reaction of imine, structure D, with N^5-($HOCH_2$)$PPTH_{2_T}$ to give a dimer with an N^5-CH_2-O-CH_2-$N^{5'}$ linkage. Formation of an N^5-CH_2-$N^{5'}$ dimer by reaction of imine with $PPTH_{2_T}$ is not likely, however, because of the large excess of formaldehyde and absence of $PPTH_{2_T}$ following the initial burst in PPT_{ox}^- formation. Reaction of imine with hydrated formaldehyde resulting in N^5-CH_2OCH_2OH substitution could occur especially if the N^1 and N^9 positions are blocked, removing the stabilizing influence of the negative charge in the uracil ring, eq 6, Structure D. The interaction of formaldehyde with the N^1 of uracil has been studied and found to occur only with neutral uracil (indistinguishable from uracil anion + H^+) with a K_{eq} = 1.[22] The formation of an N^1-carbinolamine adduct of PPT_{ox}^- (loc. cit., Scheme III) has been established. It is reasonable to suppose that N^1- and N^9-carbinolamine adducts could also occur in the reduced system, structure F. The rate-determining step(s) for termination of


F

PPT_{ox}^- formation (k_3, eq 5) is (are) likely to involve dimerization of the N^5-imine (structure E) or the reaction of the N^5-

(21) Eberlein, G.; Bruice, T. C. *J. Am. Chem. Soc.* **1982**, *104*, 1449. Hemmerich, P.; Massey, V.; Michel, H.; Schug, C. *Struct. Bonding (Berlin)* **1981**, *78*, 93.

(22) Lewin, S. *J. Chem. Soc.* **1964**, 792. Lewin, S.; Barnes, M. A. *J. Chem. Soc. B* **1966**, 478.

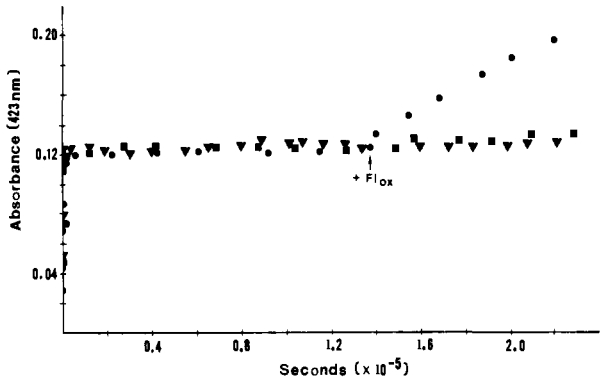

Figure 6. Absorbance (423 nm) vs. time plots for reduction of 0.06 M CH_2O by $PPTH_{2_T}$ (▼), on addition of 0.5 mL of 2.13×10^{-4} M PPT_{ox}^- (■), and on addition of 0.5 mL of 2.13×10^{-4} M Fl_{ox} (●) at $t = 1.4 \times 10^5$ s under anaerobic conditions in 0.33 M, pH 7.00, phosphate buffer at 30 °C.

carbinolamine with the N^5-imine. These structures may then react with additional formaldehyde in a non-rate-determining fashion, producing the linkages described above.

In the reaction of 1,5-dihydroflavin with formaldehyde, oxidized flavin acts as a catalyst to convert N^5-$(HOCH_2)FlH$ to FlH_2 plus CH_2O.[8] From simulation of the time course (and other experiments) the mechanism for this reaction has been established to involve oxidation of flavin formaldehyde N^5-carbinolamine by oxidized flavin (see Discussion). In order to determine if PPT_{ox}^- is a catalyst for the regeneration of $PPTH_2$ from its formaldehyde adducts, 0.5 mL of a PPT_{ox}^- solution (2.13×10^{-4} M) was tipped into reaction solutions initially 1×10^{-5} M in $PPTH_2$ and 0.06 M in CH_2O at given times (initiation of reaction, 50% completion of initial burst, and at the time of termination of PPT_{ox}^- formation). In no case did addition of PPT_{ox}^- influence the kinetics of the reaction (Figure 6). When, however, oxidized flavin replaced PPT_{ox}^-, a catalysis of the reaction of $PPTH_{2_T}$ with CH_2O was observed (Figure 6). This result finds an explanation in the more positive redox potential of Fl_{ox} as compared to that of PPT_{ox}^-.[1]

The reaction of $PPTH_{2_T}$ with *m*-hydroxybenzaldehyde (MHB) was studied under anaerobic conditions (1.0 M acetate buffer, $\mu = 1.0$) only at pH 5.00 under the pseudo-first-order conditions of [MHB] (5.36×10^{-2} to 9.52×10^{-4} M) $\gg$ [$PPTH_{2_T}$] (1×10^{-5} M). Following an initial burst in PPT_{ox}^- formation (423 nm) there occurred a continuous production of PPT_{ox}^- to completion of reaction. A quantitative description of the reaction would require computer fitting of the multiphasic time dependence for PPT_{ox}^- formation to a kinetically competent reaction sequence. This has been done previously for the reaction of 1,5-dihydro-3-methyllumiflavin with pyruvic acid, pyruvamide, ethyl pyruvate, and formaldehyde.[7,6] It suffices for the present purposes to point out that the time course for PPT_{ox}^- formation may be divided empirically into four segments which consist of three consecutive first-order processes followed by a reaction apparently zero order in PPT_{ox}^- formation. The initial reaction is seen only at high concentrations of MHB (at 3.46×10^{-2} to 5.36×10^{-2} M rate constants are $\sim 10^{-3}$ s^{-1}) and accounted for ~10% of the PPT_{ox}^- (1×10^{-5} M) formed in the reaction. The empirical rate constants for the latter three phases were independent of [MHB] and possessed values of 1.9×10^{-4} s^{-1}, 3.3×10^{-6} s^{-1}, and 6.5×10^{-8} OD s^{-1}. These phases accounted for 12%, 35%, and 43%, respectively, of the total PPT_{ox}^- (1×10^{-5} M) formed in the reaction. The absorbance (423 nm) vs. time plot for the reaction of 2.24×10^{-3} M MHB with 1×10^{-5} M $PPTH_{2_T}$ is shown in Figure 7. The MHB–$PPTH_{2_T}$ adducts present during the slow phases were found to be oxidized by addition of PPT_{ox}^-. Thus, the addition of 0.5 mL of a solution 1.27×10^{-4} M in PPT_{ox}^- at $t = 1.6 \times 10^6$ s to a reaction initially containing 2.24×10^{-3} M MHB and 1×10^{-5} M $PPTH_{2_T}$ (pH 5.00, 1 M acetate buffer) resulted in a burst of PPT_{ox} formation, Figure 7. Similarly, a burst of PPT_{ox}^- formation, greater than that found in the control, was found in this system when PPT_{ox}^- was added at the start of the reaction.

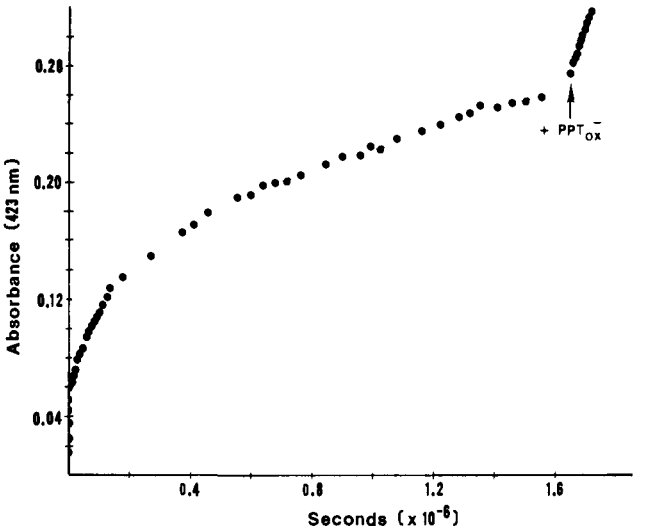

Figure 7. Plot of absorbance (423 nm) vs. time for the reaction of 2.24×10^{-3} M MHB with 1×10^{-5} M $PPTH_{2_T}$ in 1.0 M, pH 5.0, acetate buffer under anaerobic conditions. Addition of 0.5 mL of 1.27×10^{-4} M PPT_{ox}^- at $t = 1.6 \times 10^6$ s (arrow).

The product of aldehyde reduction by $PPTH_{2_T}$ was determined in a preparative experiment (see Experimental Section). The reaction of $PPTH_2$ (0.6 g, 2.04 mmol) with MBA (0.25 g, 2.04 mmol) in 50 mL of H_2O (pH 7.00, 0.33 M phosphate buffer) under anaerobic conditions at room temperature resulted in a 30% yield of *m*-cresol and 61% unreacted MBA after 1 month. The use of equivalent amounts of reactants was based on the expectation of only a two-electron transfer to give *m*-hydroxybenzyl alcohol (MBAL). Only a trace amount of MBAL was detected by gas chromatography. For verification of the identity of the major reduction product, isolation and comparison with authentic *m*-cresol were carried out. To test for the intermediacy of *m*-hydroxybenzyl alcohol (MBAL) in the formation of *m*-cresol, authentic MBAL (0.25 g, 2.01 mmol) was reacted with $PPTH_2$ (0.60 g, 2.04 mmol) under the conditions described above. No *m*-cresol was detected by gas chromatographic analysis of chloroform extracts after 2 weeks. It is concluded that the formation of *m*-cresol from MBA does not involve the intermediacy of MBAL. The reaction likely involves the reduction of a $PPTH_{2_T}$ adduct of MHB (Scheme V). An investigation of the synthetic utility of this reaction is currently under way. A preliminary finding is the ~80% conversion of MBA to *m*-cresol with formation of ~5% of MBAL when 2.5 equiv of $PPTH_2$ and 1.0 equiv of MHB are reacted at 60 °C in pH 7.0 phosphate buffer for 5 days.[23]

The observations enumerated thus far may be explained in conjunction with Scheme V and eq 11b by the following: (1) in

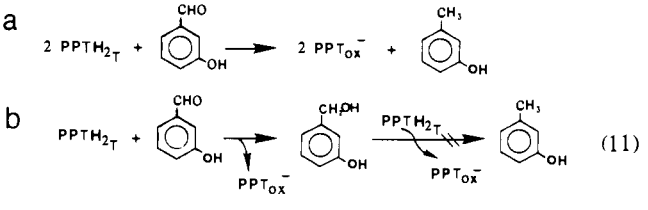

(11)

the reaction of MBA with $PPTH_{2_T}$ an initial partitioning of $PPTH_{2_T}$ to *m*-hydroxybenzyl alcohol plus PPT_{ox}^- and to MBA adducts of $PPTH_{2_T}$ occurs (both reactions are dependent upon [MBA]); (2) *m*-hydroxybenzyl PPT_{ox}^- [N^5-(MB)PPT_{ox}^-], formed from N^5-(MB=)$PPTH_{2_T}$ by a prototropic shift, is reduced by N^5-carbinolamine [N^5-(MBOH)$PPTH_{2_T}$] or $PPTH_{2_T}$ to PPT_{ox}^- and *m*-cresol (rate of reaction independent of [MBA]); (3) comproportionation of PPT_{ox}^- and adducts (eq 12) occurs to provide $PPTH_{2_T}$, which could then act as a reductant for either MBA or

(23) Bruice, T. C.; Skibo, E. B.; Venkatarm, U. V., unpublished results.

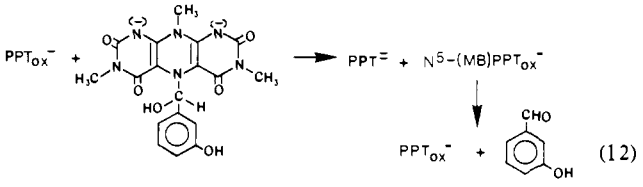

N^5-(MB)PPT_{ox}^-, leading to net formation of PPT_{ox}^- (see Figure 7). Together these processes could explain both the nature of the products and the complex multiphasic kinetics.

That the N^5-carbinolamine and N^5-imine [N^5-(MBOH)$PPTH_{2_T}$ and N^5-(MB=)$PPTH_{2_T}$, respectively] (Scheme V) are formed was determined by $NaCNBH_3$ trapping. Thus, addition of 20 mg of $NaCNBH_3$ at 8×10^5 s to a pH 5.00 (1 M acetate) solution initially containing 1×10^{-5} M $PPTH_{2_T}$ and 1.34×10^{-2} M MHB followed by addition of O_2 resulted in formation of N^5-(*m*-hydroxybenzyl)PPT_{ox}^-, N^5-(MB)PPT_{ox}^- (λ_{max} 480 nm), and its radical (λ_{max} 580 nm). Structural assignments were based on spectral comparison to the N^5-ethyl analogues (loc. cit.). The formation of N^5-(MB)PPT_{ox}^- is also predicted to occur on the pathway to *m*-cresol (Scheme V). Repetitive scanning from 700 to 350 nm of a reaction initially containing 6.17×10^{-3} M MBA and 1×10^{-5} M $PPTH_{2_T}$ in 1.0 M, pH 5.00, acetate buffer revealed only the appearance of PPT_{ox}^- at 423 nm. Perhaps N^5-(MB)PPT_{ox} never builds up as a result of its rapid reduction. Further evidence for the presence of adducts is the kinetics for the slow formation of PPT_{ox}^- when O_2 is admitted to the reaction solutions of $PPTH_{2_T}$ and MBA. Thus, addition of oxygen at 2.5×10^5 s to a reaction initially containing 1×10^{-5} M $PPTH_{2_T}$ and 8.66×10^{-3} M MHB in pH 5.00, 1 M acetate buffer resulted in PPT_{ox}^- formation to 100%. The observed absorbance (423 nm) vs. time course of reoxidation is shown in Figure 8.

The admittance of O_2 to reaction solutions containing initially $PPTH_{2_T}$ and MHB, after completion of the initial burst in PPT_{ox}^- formation, leads to a biphasic reoxidation of $PPTH_2$ adducts of MHB to PPT_{ox}^-. A very rapid formation of PPT_{ox}^- is followed by a lag phase which is followed by a slow phase ($k_{obsd} = 5 \times 10^{-3}$ s^{-1}). In order to explain these observations the following rationale is presented. The N^5-carbinolamine, N^5-(MBOH)$PPTH_{2_T}$, is oxygen sensitive and is rapidly oxidized to PPT_{ox}^-. Another species, perhaps the imine N^5-(MB=)$PPTH_{2_T}$ (written in the oxazolidine form, eq 13), reoxidizes only after conversion to its radical (an

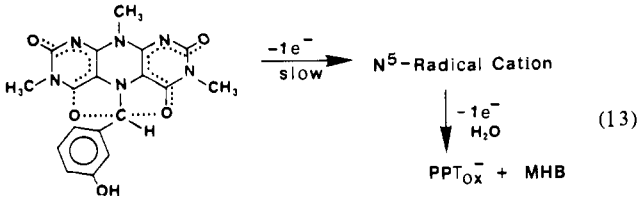

$X \rightarrow Y \rightarrow PPT_{ox}^-$ mechanism), and this is responsible for the lag period prior to the slower formation of PPT_{ox}^-. The formation of a cross-linked species, e.g. structure E, or tricarbinolamines, e.g., structure F, as postulated with formaldehyde, would not be likely because of the steric bulk of MHB. The major adducts therefore would be the N^5-imine and its carbinolamine. Supportive of the formation of adducts of low stability is the lack of complete termination of the reaction and the presence of PPT_{ox}^--mediated catalysis of the oxidation of $PPTH_2$ by MHB (loc. cit.).

The reduction of cystine and dithiodiglycolic acid to the respective mercaptans by PPT^{2-} was investigated at pH 7.00 and pH 8.00 under anaerobic conditions (30 °C, aqueous solution, phosphate buffer, $\mu = 1.0$). The formation of PPT_{ox}^- (λ 423 nm) proceeded to 90–100% yield based upon the initial [PPT^{2-}]. Mercaptans were formed in 90–100% of theory as measured with 5,5′-dithiobis(2-nitrobenzoic acid) at pH 8.00 (see Experimental Section). The kinetics for the appearance of PPT_{ox}^- were found to be sensitive to the presence of heavy metal ion impurities normally found in the reagent-grade buffer and KCl employed to maintain a constant pH. Meaningful kinetic results could not be obtained without removing these trace metal ion impurities.

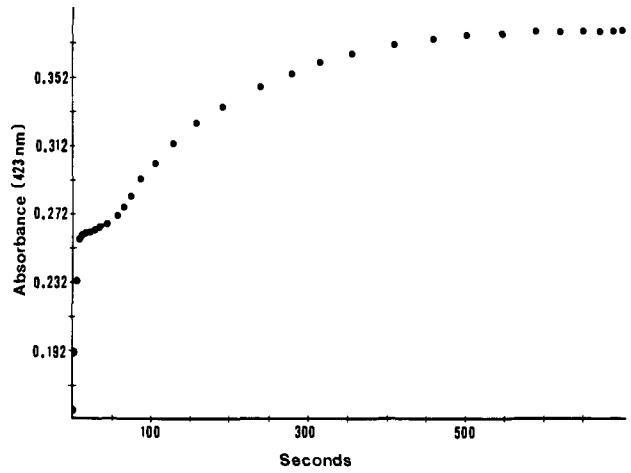

Figure 8. Absorbance (423 nm) vs. time plot for O_2-mediated oxidation of MHB adducts formed on reaction of 8.66×10^{-3} M MHB with 1×10^{-5} $PPTH_{2_T}$ in pH 5.00, 1 M acetate buffer at 30 °C. Oxygen was added at $t = 2.5 \times 10^5$ s; $OD_{423} = 0.152$ for PPT_{ox}^- formed by the reduction of MHB at this time.

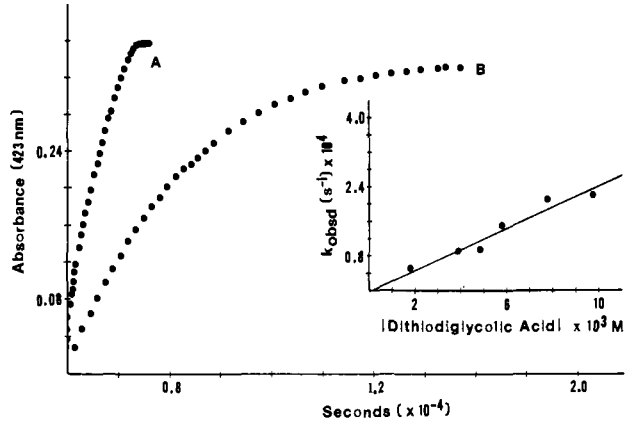

Figure 9. Absorbance vs. time plots for the reduction of 9.71×10^{-3} M dithiodiglycolic acid by 1×10^{-5} M $PPTH_{2_T}$ in untreated (A) and metal-free (B) 0.33 M, pH 7.00, phosphate buffer at 30 °C. The inset is a plot of k_{obsd} vs. [dithiodiglycolic acid] obtained with metal-free 0.33 M, pH 7.00, phosphate buffer.

Scheme V

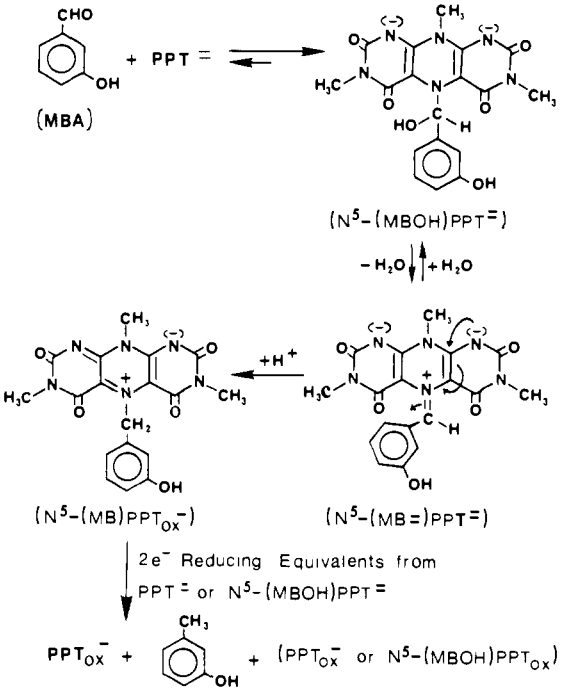

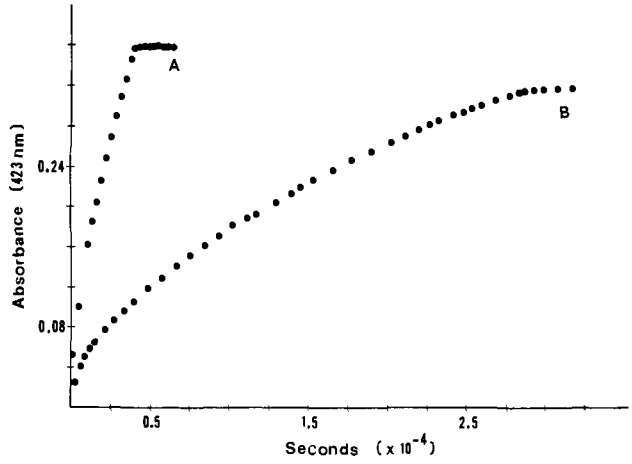

Figure 10. Absorbance vs. time plots for the reduction of 5.2×10^{-3} M cystine by 1×10^{-5} M PPT^{2-} in untreated (A) and metal-free (B) 0.33 M phosphate buffer at 30 °C and pH 7.0.

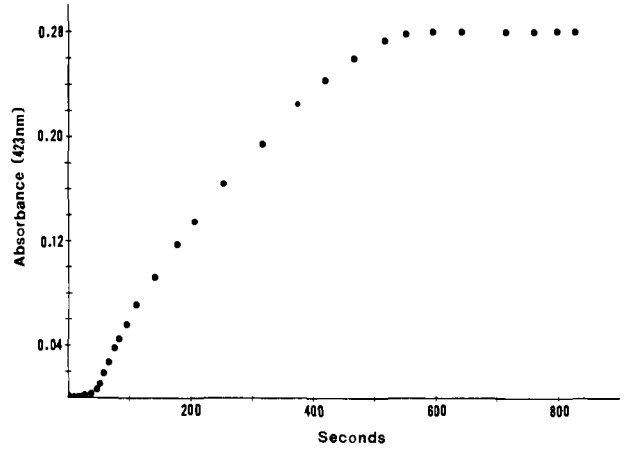

Figure 11. Absorbance (423 nm) vs. time plot for the reduction of 5.2×10^{-3} M cystine by 1×10^{-5} M $PPTH_2$, in the presence of 1.34×10^{-4} M Zn^{2+} in previously metal-free 0.33 M, pH 7.00, phosphate buffer.

The influence of metal ion impurities is shown in the experimental results exhibited in Figure 9.

Plot A of Figure 9 is the time course for the reaction of dithioglycolic acid with PPT^{2-} under the pseudo-first-order condition of [disulfide] (9.71×10^{-3} M) $\gg$ [PPT^{2-}] (1×10^{-5} M) in 0.33 M phosphate buffer at pH 7.00 when no precautions had been taken to remove trace heavy metal ions from the salts employed to prepare the buffer. In comparison, plot B of Figure 9 represents the time course for an identical experiment employing "heavy metal free" conditions. Plot B of Figure 9 follows the first-order rate law to $3t_{1/2}$. The inset to Figure 9 is a plot of the pseudo-first-order rate constant for PPT_{ox}^- appearance vs. [disulfide]. The slope of this plot is the second-order rate constant for reduction of the disulfide by PPT^{2-} (eq 14).

$$\text{S}^{-}\text{CH}_2\text{CO}_2^- \\ \text{S}^{-}\text{CH}_2\text{CO}_2^- + \text{PPT}^{=} \xrightarrow[\text{pH 7.0}]{2 \times 10^{-2}\ \text{M}^{-1}\text{s}^{-1}} 2\ \text{HSCH}_2\text{CO}_2^- + \text{PPT}_{ox}^- \qquad (14)$$

When a disulfide substrate is employed which can chelate metal ions, there is observed a heightened sensitivity of the disulfide reduction by PPT^{2-} to metal ion impurities. Cystine represents such a substrate. The time course for appearance of PPT_{ox}^- in the oxidation of PPT^{2-} (1×10^{-5} M in pH 7.00 phosphate buffer) by cystine (5.2×10^{-3} M) with and without metal-free conditions is shown in Figure 10. Plot A represents a reaction where no trace metal ions have been removed from reagents while for plot B the buffer solution has been extracted with dithiazone dissolved in CCl_2H_2 (see Experimental Section). Although plot B approaches first-order behavior, one feature of plot A, abrupt termination of absorbance time plots, is still seen. Since the cystine stock is at ~pH 10, effective demetalization is not possible and may therefore be a source of trace metal ions. Although Zn^{2+} at pH 7.0 has no influence on the reduction of dithioglycolic acid (Zn^{2+} exists as a hydrate at pH 7.0), the inclusion of $ZnSO_4$ (1.34×10^{-4} M) in a reaction (pH 7.0, phosphate buffer) containing cystine (5.2×10^{-3} M) and PPT^{2-} (1×10^{-5} M) results in a very rapid production of PPT_{ox}^-. The time course for PPT_{ox}^- formation exhibits a decided lag phase (Figure 11).

Table III. Observed Rates (s^{-1}) for the Reduction of Nicotinamides by 1×10^{-5} M $PPTH_2$ in 0.3 M Phosphate Buffer, pH 7.00, $\mu = 1.0$ KCl, at 30 °C under Anaerobic Conditions

N-benzylnicotinamide		NAD⁺	
[nicotinamide] $\times 10^3$	k_{obsd} (s^{-1}) $\times 10^4$	[nicotinamide] $\times 10^3$	k_{obsd} (s^{-1}) $\times 10^4$
4.10	9.28	2.86	9.78
2.05	5.31	2.14	7.73
1.53	2.86	1.43	5.23
1.02	2.56	0.715	2.64
0.512	1.32	0.572	1.75
0.205	0.435	0.286	1.29

The reduction of *N*-alkylnicotinamides by PPT^{2-} has been studied (30 °C, aqueous solvent) under the pseudo-first-order conditions of 2×10^{-4} M to 3×10^{-3} M *N*-alkylnicotinamide and 1×10^{-5} M PPT^{2-} in 0.33 M phosphate buffer at pH 7.0. Formation of PPT_{ox}^- (423 nm) was quantitative based upon initial [PPT^{2-}]. The reactions were found to follow the first-order rate law to completion. Plots of the pseudo-first-order rate constants (Table III) vs. [*N*-alkylnicotinamide] provide as slopes the second-order rate constants for *N*-alkylnicotinamide reduction (eq 15, 16). For the reactions of eq 15 and 16 irreversible general

$$\text{NAD}^+ + \text{PPT}^{=} \xrightarrow{0.33\ \text{M}^{-1}\text{s}^{-1}} \text{NADH} + \text{PPT}_{ox}^- \qquad (15)$$

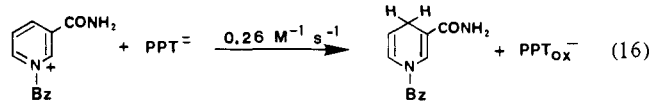

(16)

and specific acid catalyzed 5,6-hydration of the *N*-alkyl-1,4-dihydronicotinamide products must be considered[14] (eq 17). *N*-

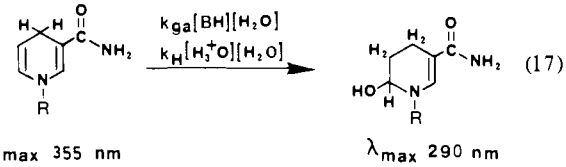

(17)

Benzyl-1,4-dihydronicotinamide (2.07×10^{-3} M) is converted to its hydrate (λ_{max} 290 nm) with the pseudo-first-order rate constant 9×10^{-5} s^{-1} (pH 7.00, 0.33 M phosphate buffer). Preparative reduction of *N*-benzylnicotinamide bromide by PPT^{2-} at pH 7.0 (see Experimental Section) yielded a product whose spectral properties were consistent with that of the 5,6-hydrate of *N*-benzyl-1,4-dihydronicotinamide. Verification of the direct reduction of *N*-alkylnicotinamide by PPT^{2-} was sought by the use of the *N*-alkylnicotinamide mimic *N*-benzylquinoline-3-carboxamide. It is not possible for the reduced form (1,4-dihydroquinoline-3-carboxamide) to undergo hydration.[15] *N*-Benzylquinoline-3-carboxamide (3×10^{-4} M) in 0.33 M phosphate buffer (pH 7.0) at 30 °C under anaerobic conditions oxidizes PPT^{2-} (1×10^{-5} M) on mixing. The percentage yield of PPT_{ox}^- was determined spectrophotometrically (423 nm) as 100% based upon initial [PPT^{2-}]. The identity of *N*-benzyl-1,4-dihydroquinoline-3-carboxamide was obtained from a preparative experiment, and it was shown to be formed in 100% yield (Experimental Section).

Discussion

The Reactions of Formaldehyde and *m*-Hydroxybenzaldehyde (MHB) with the Low Potential 1,5-Dihydroflavin Mimic 3,7,10-Trimethyl-(1*H*,3*H*,5*H*,7*H*,9*H*,10*H*)-pyrimido[5,4-*g*]pteridine-

2,4,6,8-tetrone ($PPTH_2$) Have Been Investigated. The kinetics of the reaction of $PPTH_2$ with CH_2O have been studied in detail. For the particulars of this investigation the reader is directed to Results. The chemistry involved in the reactions of the dihydropyrimido[5,4-*g*]pteridinetetrone ($PPTH_2$) and dihydroflavin (FlH_2) with carbonyl substrates may be compared. In previous studies from this laboratory there are described the reactions of dihydroflavins with pyruvic acid and derivatives and with formaldehyde.[7,8] 1,5-Dihydroflavins exist as neutral and anionic species (eq 18) while the 1,5-dihydropyrimido[5,4-*g*]pteridinetetrone of

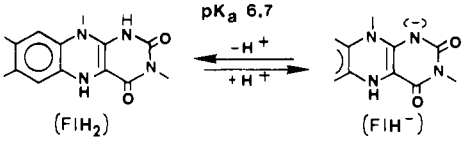

(18)

the present study exists primarily as a neutral or dianionic species (eq 19).[1] Dependent upon pH, the total 1,5-dihydroflavin (FlH_{2_T})

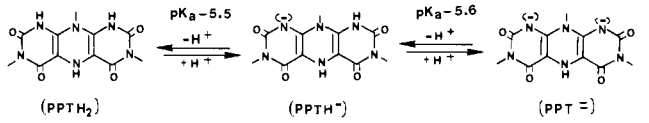

(19)

or total 1,5-dihydropyrimido[5,4-*g*]pteridinetetrone ($PPTH_{2_T}$) will exist in solution at defined mole fractions of acid and base species (FlH_{2_T} = FlH_2 + FlH^- and $PPTH_{2_T}$ = $PPTH_2$ + $PPTH^-$ + PPT^{2-}).

Kinetic investigations of the pH dependence of the reduction of carbonyl compounds by FlH_{2_T} are compatible with the more facile reaction involving H_3O^+ catalysis of the reaction of the FlH^- species with the carbonyl moiety (see particularly ref 7). For the reaction of $PPTH_{2_T}$ with CH_2O, the results are compatible with an unassisted reaction of $PPTH^-$ with CH_2O or the kinetically indistinguishable H_3O^+-catalyzed reaction of PPT^{2-} with CH_2O. If the mechanism were to involve only the reaction of $PPTH^-$ with CH_2O, it would be required that PPT^{2-} be unreactive with formaldehyde. This possibility cannot be accepted because the redox potential for the formation of PPT^{2-} by two-electron reduction of PPT_{ox}^- is more negative than the similar potential for the formation of FlH^- from Fl_{ox} by 148 mV. The species PPT^{2-} is, therefore, a much better reducing agent than FlH^- and also a better reducing agent than is $PPTH^-$. The correct mechanism for reaction of $PPTH_{2_T}$ with CH_2O must, therefore, involve specific acid catalysis of the reaction of CH_2O with the diionic species PPT^{2-}.

The reaction of FlH_{2_T} and $PPTH_{2_T}$ with carbonyl compounds is complex. These reactions share the common features: (i) In an initial burst of Fl_{ox} and PPT_{ox}^- formation, there is involved the partitioning of FlH^- and PPT^{2-} between Fl_{ox} and PPT_{ox}^- and their respective N^5-carbonyl addition products (eq 20). This partitioning involves a competition between nucleophilic attack by the N^5-amino nitrogens of FlH^- and PPT^{2-} upon the carbonyl carbon and reduction of the carbonyl function by electron transfer[7,8] (we will return to these competitive reactions shortly). (ii) Formation of N^5-CA_F is thermodynamically favored in the reaction of FlH^- with CH_2O and the rate of return is slow, effectively terminating the initial burst. In the reaction of $PPT^=$ with CH_2O, the formation of the N^5-CA_p involves a rapid equilibrium and the burst is terminated by formation of the highly stable N^5-imine (structure D). (iii) Continual slow formation of Fl_{ox} and PPT_{ox}^- by reversal of N^5-carbinolamine or N^5-imine formation is further slowed (as with PPT^{2-} reacting with MHB and FlH^- reacting with CH_2O) or terminated (as in the reaction of PPT^{2-} with CH_2O) by the formation of further condensation products of N^5-CA and derived N^5-IM species with carbonyl reagent (ex. Results species E and F). (iv) The redox reaction products Fl_{ox} and PPT_{ox}^- may act as catalysts for the reduction of carbonyl compounds by FlH^- and PPT^{2-} by a redox reaction which regenerates free FlH_2 and $PPTH_2$ (eq 21). The reactions of eq 21a are observed in the reduction

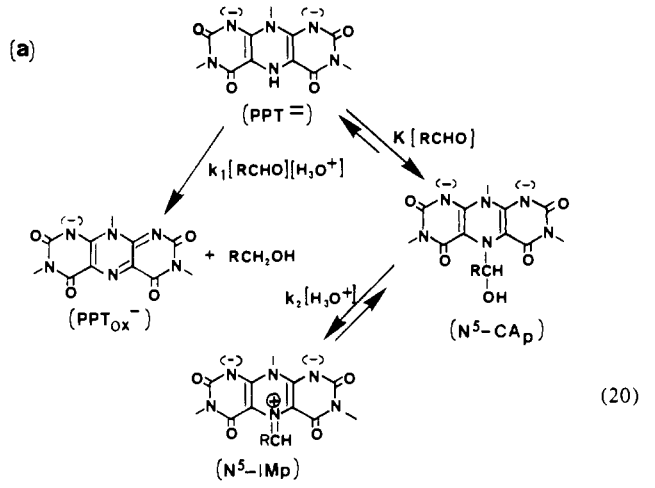

(20)

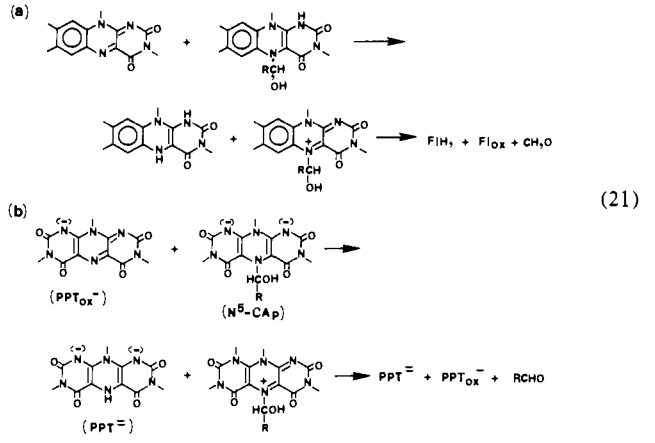

(21)

of CH_2O, $CH_3COCO_2^-$, CH_3COCO_2H, CH_3COCO_2Et, and $CH_3COCONH_2$ by FlH_2.[7,8] The reaction of eq 21b does not occur with PPT^{2-} and CH_2O, but it is seen in the reaction of PPT^{2-} with MHB. The PPT_{ox}^- is not as good an oxidant as is Fl_{ox}. This is shown by the fact that Fl_{ox} will oxidize the N^5-CA_p species formed from both CH_2O and MHB. The inability of PPT_{ox}^- to oxidize the N^5-CA_p of CH_2O must reside in the more negative potential for two-electron transfer to this species as compared to that of the N^5-CA_p species generated from MHB.

The two-electron reduction potential for $Fl_{ox} \rightarrow FlH^-$ at pH 7.0 is −198 mV[24] whereas the two-electron reduction potential for $PPT_{ox}^- \rightarrow PPT^{2-}$ is 346 mV.[1] The hydrogen ion catalyzed reduction of CH_2O by FlH^- is associated with the rate constant 2.3×10^4 M^{-2} s^{-1} [8] while the similar constant for PPT^{2-} reduction of CH_2O has been determined to be 3.3×10^6 M^{-2} s^{-1}. The logarithmic difference ($\Delta \log k_i$) in these rate constants amount to 2.15. The difference in the two-electron reduction potentials of Fl_{ox} and PPT_{ox}^- is 148 mV. It follows that the increase in the

(24) Draper, R. D.; Ingraham, L. L. *Arch. Biochem. Biophys.* **1968**, *125*, 802.

rate of reduction of formaldehyde obtained by exchanging FlH^- by PPT^{2-} follows the relationship 67 mV/Δ log k_i. From the Nernst equation, a plot of the log of the rate constants vs. E_o' for a two-electron reduction by a series of 1,5-dihydroflavins should be linear and of slope 60 mV/Δ log k_N. Thus, the second-order rate constant for reduction of CH_2O by PPT^{2-} is that expected of a 1,5-dihydroflavin possessing the redox potential of PPT^{2-}.

Arguments have been presented (based upon electrochemical and kinetic data) that the reduction of carbonyl compounds by FlH^- represents sequential two-electron transfer processes.[7] In the reaction of FlH^- with CH_2O the ratio of Fl_{ox}:N^5-CA_F (reaction a and b of eq 20) is 2:1. In the reaction of PPT^{2-} with CH_2O the ratio of PPT_{ox}^-:N^5-IM_p is 4:1. It follows that the difference in the free energies of activation for CH_2O reduction and carbinolamine formation is only 1.7 kJ M^{-1} for FlH^- and less than 3.4 kJ M^{-1} for PPT^{2-}. On a free energy scale, the rate for N^5-carbinolamine formation shows the same sensitivity to the change of reduction potential as does the rate for CH_2O reduction. This interesting observation may simply reflect a like dependence of the nucleophilicity of the N^5-position and redox potential on structure. On the other hand, both carbonyl function reduction and nucleophilicity may involve electron transfer. The formation of the N^5-carbinolamine may be an example of nucleophilic attack with one-electron transfer leading.[25]

In the reaction of $PPTH_{2_T}$ with MHB the initial reaction (eq 20a), which yields ~90% N^5-IM_p and ~10% *m*-hydroxybenzyl alcohol, is followed by slower formation of PPT_{ox}^- to 100% yield based on the initial [$PPTH_{2_T}$]. The overall time course resembles that for reaction of pyruvic acid–pyruvate with FlH_{2_T} at certain pH values.[7] In this instance both the initial reaction and the following slower formation of Fl_{ox} result in lactic acid–lactate formation.[7] In the instance of the reaction of $PPTH_{2_T}$ with MHB, the slow formation of PPT_{ox}^-, following the initial burst, is not accompanied by *m*-hydroxybenzyl alcohol formation. The product of this reaction is *m*-cresol. The mechanism of this reaction is not understood; however, *m*-hydroxybenzyl alcohol is not an intermediate. The stoichiometry of the reaction requires that 2 equiv of $PPTH_{2_T}$ is involved in the reduction of 1 equiv of MHB (eq 11). We are unaware of any organic reagent capable of reducing an aldehyde to a hydrocarbon in aqueous media much less one that can do so without generating an alcohol as an intermediate. The mechanism of Scheme V is offered as being plausible. The problem is under continuing study.[23]

The reduction of the disulfide bonds of cystine and dithiodiglycolic acid by PPT^{2-} has been determined to be first order in the disulfide and first order in PPT^{2-}. These reactions were studied over a narrow pH range and the influence of buffer acid and base species were not assessed. A considerable effort has been expended in the study of mercaptan oxidation by flavins. In this regard the investigations of Loechler and Hollacher[4e] must be considered as heroic. The mechanism of eq 22 has received common support.[4] Though reduction of alkyl disulfides by 1,5-dihydroflavins has not been shown, the mechanism of eq 22 requires that it occur by nucleophilic attack of the 4a-position of the dihydroflavin upon sulfur. A priori, this same mechanism would be anticipated for

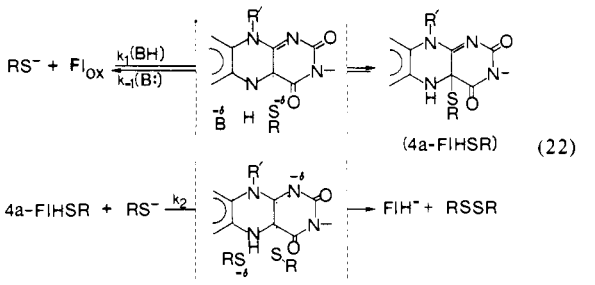

(22)

disulfide bond reduction by PPT^{2-}. If nucleophilic attack of PPT^{2-} upon the disulfide bond were rate determining, then general catalysis would not be anticipated. However, if dissociation of the 4a-thiol adduct were rate determining, general base catalysis should be observed. An investigation of the details of the reduction of organic disulfides by $PPTH_{2_T}$ is presently under investigation in this laboratory.

Reduction of dithiodiglycolic acid and particularly cystine by PPT^{2-} is assisted by the presence of trace metal ions. One might envision metal ion assistance to the nucleophilic attack of PPT^{2-} upon the disulfide bond and also in the decomposition of any 4a-thiol adduct.

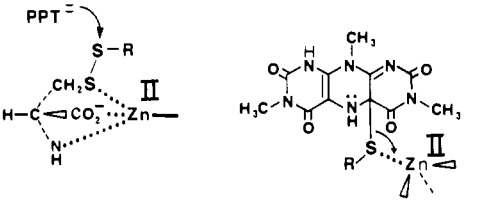

The bimolecular reaction of $PPTH_{2_T}$ with *N*-alkylnicotinamides leads to the quantitative formation of PPT_{ox}^- and *N*-alkyl-1,4-dihydronicotinamides. Present evidence[26] suggests that Fl_{ox} reduction by *N*-alkyl-1,4-dihydronicotinamides involves the transfer of H^- from the dihydronicotinamide moiety to Fl_{ox}. Presumably the same mechanism is involved in the reduction of nicotinamides by $PPTH_{2_T}$.

The possibility that a pyrimido[5,4-*g*]pteridine may serve as a redox cofactor in some, as yet not at all characterized, enzymatic reaction deserves consideration. This suggestion is based on the establishment in this laboratory of the catalytic redox properties of $PPTH_2$ and the fact that the 5-amino-2,4-dioxy-6-ribitylaminopyrimidine (ADRAP) required for any biochemical synthesis of the pyrimido[5,4-*g*]pteridine is an intermediate in the biosynthesis of riboflavin.[27] The self-condensation of diaminouracils is known, and Cresswell, Neilson, and Wood[27] have shown that ADRAP self-condenses in a nonenzymatic reaction (eq 23).

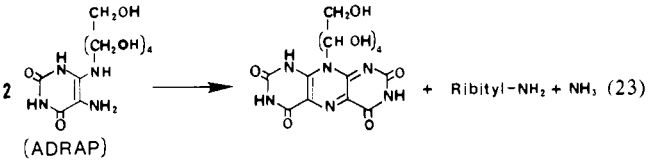

(23)

It will be of interest to determine if the 10-ribitylpyrimido-[5,4-*g*]pteridine product of eq 1 is subject to 5′-phosphorylation and conversion to pyrimido[5,4-*g*]pteridine–adenosine dinucleotide by the flavokinase–FAD synthetase complex of *Brevibacterium ammoniagenes*[29] so that it could be studied both as a flavin mononucleotide and dinucleotide mimic in enzymatic reactions.

Acknowledgment. This work was supported by the National Institutes of Health and the National Science Foundation.

(25) For examples of nucleophilic reactions that are proposed to be radical in nature, see: (a) Russell, G. A.; Norris, R. K.; Panek, E. J. *J. Am. Chem. Soc.* **1971**, *93*, 5389. Russell, G. A.; Danen, W. C. *Ibid.* **1966**, *88*, 5663. Russell, G. A.; Janzen, E. G.; Strom, E. T. *Ibid.* **1964**, *86*, 1807. (b) Kornblum, N.; Davies, T. M.; Earl, G. W.; Greene, G. S.; Holy, N. L.; Kerber, R. C.; Manthey, J. W.; Musser, M. T.; Snow, D. H. *Ibid.* **1967**, *89*, 5714. (c) Bunnett, J. F.; Floor, B. F. *J. Org. Chem.* **1974**, *39*, 382. (d) Bank, S.; Noyd, D. A. *J. Am. Chem. Soc.* **1973**, *95*, 8203. (e) Bilevitch, K. A.; Okhlobystin, O. Yu. *Russ. Chem. Rev. (Engl. Transl.)* **1968**, *37*, 954. (f) Bilevitch, K. A.; Pubnov, N. N.; Okhlobystin, O. Yu. *Tetrahedron Lett.* **1968**, 3465. (g) Zoltewicz, J. A.; Oestreich, T. M. *J. Am. Chem. Soc.* **1973**, *95*, 6863. (h) Misra, H. P. *J. Biol. Chem.* **1974**, *249*, 2151. (i) Tokumaru, K.; Simamura, O. *Bull. Chem. Soc. Jpn.* **1963**, *36*, 333. (j) Chalfont, G. R.; Perkins, M. J. *J. Chem. Soc. B* **1971**, 245. (k) Kosower, E. M. "Physical Organic Chemistry"; Wiley: New York, 1968; 163ff, 179ff. (l) Garst, J. F. In "Free Radicals", Kochi, J. D., Ed.; Wiley: New York, 1973; Vol. 1, 503ff. (m) Chung, S.-K.; Chung, F.-T. *Tetrahedron Lett.* **1979**, 2473. (n) Chung, S.-K. *J. Org. Chem.* **1980**, *45*, 3513. (o) Abe, T.; Ihagami, Y. *Bull. Chem. Soc. Jpn.* **1976**, *49*, 3227. (p) Pryon, W. A. *J. Am. Chem. Soc.* **1975**, *97*, 1580.

(26) Powell, M. F.; Wong, W. H.; Bruice, T. C. *Proc. Natl. Acad. Sci. U.S.A.* **1982**, *79*, 4604. Powell, M. F.; Bruice, T. C. *J. Am. Chem. Soc.* **1982**, *104*, 5834. Powell, M. F.; Bruice, T. C. *Ibid.* **1983**, *105*, 1014.

(27) Hollander, I. J.; Braman, J. C.; Brown, G. M. *Biochem. Biophys. Res. Commun.* **1980**, *94*, 515. See also the many studies of G. W. E. Plant and collaborators.

(28) Cresswell, R. M.; Neilson, T.; Wood, H. C. S. *J. Chem. Soc.* **1960**, 4776.

(29) Spencer, R.; Fisher, J.; Walsh, C. *Biochemistry* **1976**, *15*, 1043.

Registry No. PPTox, 82639-45-0; $PPTox^-$, 82639-46-1; $PPTH_2$, 82639-48-3; PPT^{2-}, 82639-47-2; N^5-$EtPPTH_2$, 85222-30-6; N^5-$EtPPT^-$, 85249-96-3; N^5-EtPPTox, 82639-50-7; N^5-MePPTox, 85222-31-7; N^5-EtPPT-4α-OH, 82639-52-9; acetaldehyde, 75-07-0; formaldehyde, 50-00-0; *m*-hydroxybenzaldehyde, 100-83-4; cysteine, 52-90-4; dithiodiglycolic acid, 505-73-7; *N*-benzylnicotinamide, 2503-55-1; *N*-benzyl-1,4-dihydro-3-quinolinecarboxamide, 17260-79-6; nicotinamide adenine dinucleotide, 53-84-9; $NaCNBH_3$, 25895-60-7.

Kinetic Studies of Intramolecular Excimer Formation in Dipyrenylalkanes

M. J. Snare, P. J. Thistlethwaite,* and K. P. Ghiggino

Contribution from the Chemistry Department, Melbourne University, Parkville, Victoria 3052, Australia. *Received May 24, 1982*

Abstract: The kinetics of excimer formation in 1,3-bis(1-pyrenyl)propane and 1,10-bis(1-pyrenyl)decane have been studied in a range of solvents. In neither case does the excimer formation rate show a marked dependence on solvent bulk viscosity. In the case of 1,3-bis(1-pyrenyl)propane the results indicate two initial conformation groups that on excitation form the excimer with different average rate constants.

Introduction

Dipyrenylalkanes are suitable for the investigation of intramolecular excimer formation. It is known that, in addition to a structured monomer fluorescence band with a maximum near 375 nm, the emission spectra of these compounds exhibit a broad, structureless band with maximum intensity in the vicinity of 480 nm, which is due to fluorescence from intramolecular excimers.[1] Two features of pyrene account for this intramolecular excimer formation and the consequent suitability of pyrene (Py) as a probe for studying the kinetics of conformational change in alkanes. First, the stabilization energy of pyrene excimers is large (0.34 eV in cyclohexane).[2] This means that if an excited and a ground-state pyrene achieve the appropriate configuration, then the excimer readily forms and there is little tendency for subsequent dissociation. Second, the long fluorescence lifetime of pyrene derivatives increases the chance of a suitable configuration being attained within the excited pyrene lifetime. Studies have been undertaken using steady-state measurements of fluorescence intensities in the series pyrene-$(CH_2)_n$-pyrene with n = 2-16 and 22 in methylcyclohexane.[1] While several investigations have made use of the relative intensities in the monomer and excimer regions,[3-5] fewer direct kinetic treatments have been reported.[6] Intramolecular excimer emission is strongest for dipyrenylpropane, which has been used as a fluorescent probe for micellar interiors. It has been clamined that the excimer formation rate decreases essentially linearly with increasing viscosity in highly viscous solvents.[4] However, doubts as to the validity of using dipyrenylpropane as a probe of microviscosity have been raised.[5]

The interaction between an excited and a ground-state pyrene chromophore linked by an alkane chain can be represented by the familar Scheme I,[7] where k_{1M} and k_{FM} are respectively the radiationless and radiative decay rates of the excited pyrene monomer and k_{1D} and k_{FD} are the corresponding rates for the excimer. Kinetic analysis of the photostationary situation yields for the ratio of the excimer and monomer emission intensities

Scheme I

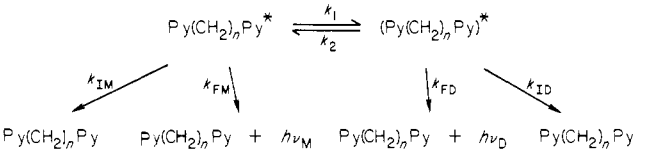

$$\frac{I_{ex}}{I_{mon}} = \frac{k_1\tau_D}{1 + k_2\tau_D}\frac{k_{FD}}{k_{FM}}$$

where $\tau_D = (k_{FD} + k_{1D})^{-1}$. For the steady excimer to monomer emission intensity ratio to be a measure of viscosity requires, in the most general case, that k_1, k_2, τ_D, k_{FD}, and k_{FM} all depend only on viscosity. It has already been shown that at least one of those constants does not comply with this condition.[5] Two simplifying assumptions can be envisaged for the above scheme. In the first, $k_2\tau_D \ll 1$ and thus

$$I_{ex}/I_{mon} \simeq k_1\tau_D k_{FD}/k_{FM}$$

In the second (excited-state equilibrium) $k_2\tau_D \gg 1$ and

$$I_{ex}/I_{mon} \simeq (k_1/k_2)(k_{FD}/k_{FM})$$

Although it seems likely that the radiative rate ratio, k_{FD}/k_{FM}, would be approximately independent of solvent, it is much less certain that the remaining constants depend only viscosity. Rate constants for excimer formation and dissociation in methylcyclohexane have already been reported,[6] but the method has been criticized.[5] The effect of solvent has not been studied. In this work k_1, k_2, and τ_D are determined for the compounds with n = 3 and 10 in four low-viscosity solvents. The results indicate that in the n = 10 case neither of the foregoing limiting situations applies. In the n = 3 case, although the data point to k_2 being negligible, other complications arise.

While excimer formation between free molecules in solution is diffusion controlled, departures from this behavior might be expected in constrained systems where the chromophores are linked by short alkane chains. In a study of intramolecular excimer formation and dissociation, Johnson reported that for 1,3-bis(*N*-carbazolyl)propane, in a group of chemically and structurally

(1) Zachariasse, K. A.; Kühnle, W *Z. Phys. Chem. (Wiesbaden)* **1976**, *101*, 267.
(2) Birks, J. B.; Dyson, D. J.; Munro, I. H. *Proc. R. Soc. London, Ser. A.* **1963**, *275*, 575.
(3) Zachariasse, K. A. *Chem. Phys. Lett.* **1978**, *57*, 429.
(4) Zachariasse, K. A.; Kühnle, W.; Weller, A. *Chem. Phys. Lett.* **1980**, *73*, 6.
(5) Henderson, C. N.; Selinger, B. K.; Watkins, A. R. *J. Photochem.* **1981**, *16*, 215.
(6) Zachariasse, K. A.; Kühnle, W.; Weller, A. *Chem. Phys. Lett.* **1978**, *59*, 375.
(7) Ghiggino, K. P.; Roberts, A. J.; Phillips, D. *Adv. Polym. Sci.* **1981**, *40*, 69.

0002-7863/83/1505-3328$01.50/0